Mycobacterium abscessus virulence traits unraveled by transcriptomic profiling in amoeba and macrophages

Violaine Dubois[1], Alexandre Pawlik[2], Anouchka Bories[1], Vincent Le Moigne[1], Odile Sismeiro[3], Rachel Legendre[3,4], Hugo Varet[3,4], Pilar Rodriguez[7], Jean-Louis Gaillard[1,5], Jean-Yves Coppée[3], Roland Brosch[2], Jean-Louis Herrmann[1,6*] and Fabienne Girard-Misguich[1*]

[1] 2I, UVSQ, INSERM, Université Paris-Saclay, Versailles, France.

[2] Unité de Pathogénomique Mycobactérienne intégrée, Institut Pasteur, Paris, France

[3] Institut Pasteur - Bioinformatics and Biostatistics Hub - C3BI, USR 3756 IP CNRS, Paris, France.

[4] Institut Pasteur - Transcriptome and Epigenome Platform - Biomics Pole - C2RT, Paris, France.

[5] APHP, GHU PIFO, Hôpital Ambroise Paré, Boulogne Billancourt, France.

[6] APHP, GHU PIFO, Hôpital Raymond Poincaré, Garches, France.

[7] Laboratoire d'Écologie, Systématique et Évolution, Université Paris-Saclay, Orsay, France

Key words: Amoeba, Macrophage, *Mycobacterium abscessus*, virulence, replication

Short title: *Mycobacterium abscessus* virulence modeled by environmental amoebae

* Correspondence: Fabienne Girard-Misguich: fabienne.misguich@uvsq.fr; Jean-Louis Herrmann: jean-louis.herrmann@aphp.fr

Abstract

Free-living amoebae might represent an evolutionary niche. In order to get more insights into the potential amoebal training ground for *Mycobacterium abscessus*, we characterized its full transcriptome in amoeba (Ac) and macrophages (Mϕ), as well as the *Mycobacterium chelonae* intra-Ac transcriptome for comparison. Up-regulated genes in Ac allowed *M. abscessus* to resist environmental stress and induce defense mechanisms, as well as showing switch from carbohydrate carbon sources to fatty acid metabolism. Eleven genes implicated in the adaptation to intracellular stress, were mutated, with all but one confirmed to be involved in *M. abscessus* intra-Mϕ survival. Cloning two of these genes in *M. chelonae* increased its intra-Mϕ survival. One mutant was particularly attenuated in Mϕ that corresponded to the deletion of an Eis N-acetyl transferase protein (*MAB_4532c*). Taken together, *M. abscessus* transcriptomes revealed the intracellular lifestyle of the mycobacteria, with Ac largely contributing to the enhancement of *M. abscessus* intra-Mϕ survival.

Introduction

To date, most of the known mycobacterial species are environmental organisms found in soil (Lavania et al., 2008), air (Angenent et al., 2005) and water (Ben Salah et al., 2009; Gomila et al., 2008; Guidotti et al., 2008), and belong to the Rapid Growing Mycobacteria (RGM). In contrast, most of the host-associated mycobacteria are slow growing mycobacteria (SGM). However, some exceptions exist. *Mycobacterium abscessus* and members of the *Mycobacterium chelonae* complex, in addition to *Mycobacterium fortuitum*, represent the main opportunistic pathogens among RGM (Griffith et al., 2007).

Identification of the last common ancestor of the genus *Mycobacterium* is still a matter of debate, although recent studies proposed the ancestor as an environmental species that evolved either as a soil-borne mycobacterium, as a waterborne mycobacterium such as *Mycobacterium avium-intracellulare* and *Mycobacterium marinum*, or as a host-associated mycobacterium such as *Mycobacterium avium* subsp *paratuberculosis* and *M. avium* subsp *avium*, *Mycobacterium tuberculosis* complex (MTBC) species and *Mycobacterium leprae* (Ahmed et al., 2007; Stinear et al., 2008).

Compared to other non-tuberculous mycobacteria (NTM), recovery of *M. abscessus* from the environment is rare (Thomson et al., 2013). Information from its genome sequence indicates its presence at the interface of soil, vegetation and water, an environment where free-living amoebae (FLA) are commonly found (Ripoll et al., 2009). FLA have been isolated from habitats in common with mycobacteria (Falkinham, 2009; Thomas and McDonnell, 2007) including cold-drinking water systems (Eddyani et al., 2008; Thomas et al., 2006), hot water systems in hospitals and cooling towers (Pagnier et al., 2008). FLA are ubiquitous organisms that feed on bacteria, and these bacteria have likely developed adaptations to the intracellular lifestyle to become amoeba-resistant bacteria (ARB) (Adékambi *et al.*, 2006; Lamrabet *et al.*, 2012). Mycobacteria have been isolated from such habitats by amoebal enrichment (Thomas et al.,

2006)(White et al., 2010), allowing potential evolution toward pathogenicity by the acquisition of virulence genes by horizontal gene transfer (Gutierrez *et al.*, 2005; Ripoll *et al.*, 2009). Finally, amoebae are often considered as an ancestral form of macrophages (Mϕ) sharing similar cellular structures and biological features (Barker and Brown, 1994; Greub and Raoult, 2004; Siddiqui and Khan, 2012).

M. abscessus has been shown to be resistant to amoeba phagocytosis and encystment, a property shared with all mycobacteria with the exception of the attenuated *M. bovis* BCG vaccine strain (Adékambi *et al.*, 2006; Salah *et al.*, 2009; Bakala N'Goma *et al.*, 2015). In addition, co-culture of *M. abscessus* with *Acanthamoeba castellanii* (Ac) increases its virulence when aerosolized in mice (Bakala N'Goma *et al.*, 2015) suggesting the existence of an amoebal 'training ground' for opportunistic pathogenic mycobacteria. Similarly, co-culture of amoebae with *M. avium* was found to trigger *M. avium* virulence by enhancing both entry and intracellular multiplication of the bacterium (Cirillo et al., 1997). The essential role of the ESX-4 *M. abscessus* type VII secretion system (T7SS) has also been demonstrated based on an intra-amoebal viability screen of *M. abscessus*, unraveling for the first time the active role of ESX-4 in intracellular *M. abscessus* survival (Laencina et al., 2018).

In order to gain more insights into the proposed amoebal training ground for *M. abscessus*, we characterized the full transcriptome of *M. abscessus* in Ac and Mϕ, as well as the *M. chelonae* intra-amoebal transcriptome for comparison and characterization of *M. abscessus* virulence adaptations to intracellular life. Although amoebae and Mϕ share common features, it has been shown that an intra-amoebal life requires specific adaptations (Laencina et al., 2018). A full description and analysis of *M. abscessus* transcriptomes will allow the identification of essential genes and a complete picture of *M. abscessus* intracellular replication and survival, whether in an amoeba environmental host or in Mϕ, and elucidation of the mechanisms employed by the bacteria to resist host responses.

Results

Overall description of the M. abscessus *intracellular transcriptomes*

RNAseq data from *M. abscessus* planktonic or intracellular cultures (3 to 4 replicates per condition) were analyzed and compared to identify *M. abscessus* genes that were up- or down-regulated after Ac and Mϕ co-cultures. Transcriptomes of *M. abscessus* in-Ac 4 and 16 hours post-infection (hpi), in Mϕ 16 hpi and transcriptomes of *M. chelonae* in Ac 16 hpi were obtained and invariant genes were excluded from the analyses. Normalization and hierarchical clustering of normalized raw date confirmed the quality of transcriptomes (**Sup. Figure 1**). Differentially expressed genes (DEGs) were identified using the *DESeq2* package (Love et al., 2014) (Sup. Table 1) and the Log_2 fold change (FC) values from *M. abscessus* transcriptomes were compared (**Sup. Figure 2**). In Ac, most DEGs up-regulated or down-regulated at 4hpi were still up- or down-regulated at 16hpi (**Figure 1A**). In order to detail the biological changes that correlated with *M. abscessus* intracellular regulation, we first grouped the DEGs in cluster of orthologues (Cluster of Orthologous Groups or COGs) (Tatusov et al., 2000). Highly up-regulated genes in Ac were more frequently found in COG O (Post-translational modification, protein turnover, chaperones), COG K (Transcription) and COG I (Lipid transport and metabolism) compared to the genome reference, although this last category tended to be under-represented at 16 hpi (**Figure 1B**). Comparatively, highly down-regulated genes were assigned to COG E and COG F (amino-acid and nucleotide transport and metabolism respectively) (**Figure 1B**).

When comparing *M. abscessus* Ac-16hpi *vs*. Mϕ-16hpi transcriptomes, DEGs were found more dispersed, with 20% of DEGs regulated in the opposite direction (increased versus decreased and vice versa) (**Figure 1C**). The representation of DEG according to their FC highlighted that in Ac and Mϕ most DEGs showed low changes (FC<|2|) 16 hpi (**Sup. Figure 2A**). In Ac, UP

regulated DEGs predominated in comparison with their behavior in a Mϕ environment (**Sup. Figure 2B**).

COG designations highlighted the differences between *M. abscessus* high DEGs in Mϕ and Ac (**Figure 1D**). COG O, which was over-represented in the *M. abscessus* highly up-regulated genes in Ac, was more frequently associated with highly down-regulated genes in Mϕ (**Figure 1B-D**). By comparison, COG P (Inorganic ion transport and metabolism) was over-represented in the *M. abscessus* transcriptome in Mϕ only, potentially illustrating different adaptations to amoebal and Mϕ environments (**Figure 1D**).

Main biological pathway changes of M. abscessus *in Ac and Mϕ*

We performed a gene ontology enrichment (GOE) analysis to further characterize the *M. abscessus* adaptions in Ac and Mϕ. GOE were qualified by an enrichment factor (EF) (1 to 4) and a number of significantly enriched genes (from small (<10) to large (>100)) (**Figure 2**). In Ac, the most enriched up-regulated *M. abscessus* genes fell into polyamine transport (GO:0015846) to adenine salvage (GO:0006168), including small groups of genes involved in sulfur metabolism (sulfate assimilation pathway (SAP) (GO:0000103), hydrogen sulfide (H2S) biosynthetic pathway (GO:0070814) and detoxification (iron-sulfur cluster assembly (GO:0016226) (**Figure 2A**).

In Mϕ, *M. abscessus* up-regulated enriched genes fall into different GO in comparison to those up-regulated in Ac. L-proline biosynthetic process (GO:0055129); methylerythritol 4-phosphate MEP pathway (GO:0019288) and Glycerol ether metabolic process (GO:0006662) were the most enriched (**Figure 2B**). These GO are followed by the type II secretion system and notably the Tat (twin-arginine translocation) pathway.

In Ac *M. abscessus* infections, the most enriched down-regulated genes fell into the nitrate assimilation GO (GO:0042128), to glycogen biosynthetic process GO (GO:0005978) (**Figure**

136 **2C**). In particular GO related to transport and metabolism of glucose were enriched
137 (GO:0005977, GO:00015749, GO:0009250, GO:0005978) (**Figure 2C**).
138 In Mϕ, *M. abscessus* down-regulated genes related to growth and parietal activities. From
139 GO:0040007 corresponding to growth, up to GO:0030259 corresponding to lipid glycosylation,
140 in addition to GO:0071941 (nitrogen cycle metabolism process), GO:0009259 (peptidoglycan
141 synthesis) and GO:0022604 (regulation of cell morphogenesis), GOE indicated that
142 *M. abscessus* slows down its energy-lycost metabolic processes and growth rate (**Figure 2D**).
143 Taken together, these observations suggest that *M. abscessus* enters a slow-replicative state in
144 Mϕ and dedicates its energy to detoxification and protein secretion into the host.
145
146 *Regulation of the central carbon metabolism of* M. abscessus in Ac and Mϕ
147 Following the GOE analysis, we investigated the different *M. abscessus* up- and down-
148 regulated genes from metabolic pathways in Ac or Mϕ. The major finding was that
149 *M. abscessus* switches from a simple sugar-based carbon source to fatty acids inside Ac and
150 Mϕ (**Figure 3**). The glycolysis/neoglucogenesis and pentose phosphate pathways were mostly
151 down-regulated or unchanged inside cells whereas the β-oxidation of fatty acids was up-
152 regulated in Ac and Mϕ. This switch was observed from the early time points after Ac infection.
153 Fifteen genes predicted to encode enzymes necessary for the biochemical activation and β-
154 oxidation of fatty acids were up-regulated in Ac and Mϕ, such as: fatty acid-coenzyme A (CoA)
155 synthase (*fadD3*, *9*, *10*, *19*); acyl-CoA dehydrogenase (*fadE5*, *14*, *23-24*, *27-29*, *31*); enoyl-
156 CoA hydratase (*echA19*); hydroxy-butyryl-CoA dehydrogenase (*fadB2*) and acetyl-CoA
157 transferase (*fadA5*, *6*). Genes implicated in the synthesis of enzymes involved in the breakdown
158 of cholesterol A and B rings were highly induced in Ac and Mϕ. β-oxidation of fatty acid and
159 cholesterol breakdown result in the accumulation of propionyl-CoA that is detoxified by the
160 methylmalonyl pathway. By-products of these 3 pathways and the GABA shunt feed the TCA

cycle. The succinate generated by the TCA cycle enables the bacterium to deal with anaerobic respiration (Hartman et al., 2014). In addition, *M. abscessus* may detoxify glyoxylate by converting it into malate via the glyoxylate shunt (**Figure 3**).

Furthermore, down-regulation of the mycolate operon (*MAB_2027-MAB_2039*) (**Table 1**), encompassing the β-ketoacyl-ACP synthases (KasA & KasB) and β-ketoacyl synthases (MAB_2031 & MAB_2029), as well as the malonyl-CoA acyl carrier protein transacylase (MCAT) homolog (MAB_2034), revealed that intracellular *M. abscessus* undergoes starvation as previously described (Jamet et al., 2015).

Regulation of putative virulence genes of M. abscessus *in Ac and Mϕ*

We assessed the regulation of *M. abscessus* genes conserved in *M. tuberculosis* that are known to be induced and to contribute to the cellular microbicidal defenses of the tubercle bacillus in Mϕ (Mukhopadhyay et al., 2012). The picture looked similar between Ac and Mϕ with a few exceptions in the response to low O_2/NO and in the low iron response (**Figure 4**). Transcriptional regulators such as *dosR*, *phoP* and *mtrA* were regulated in the opposite direction in Ac and Mϕ, with *phoP* and *mtrA* only induced in Ac, and *dosR* exclusively induced in Mϕ. Other genes known to contribute to the survival of the bacterium in response to oxidative stress (Sherman et al., 1999), comprising *ahpD*, *bcp*, *trxB1* and *2*, *trxC* genes (Schnappinger *et al.*, 2003), in addition to *ahpC*, were up-regulated in Ac and Mϕ.

Altogether, these analyses suggest that the induced sets of genes in Ac reflect the main adaptations to resistance to intracellular stress that were also shown to be induced in Mϕ, hence suggesting that they constitute a repertoire of genes participating in *M. abscessus* virulence through intra-phagocyte survival.

M. abscessus *highly-induced genes in amoeba*

186 The highest FC values of the *M. abscessus* in Ac 4 and 16hpi were chosen and then compared
187 to the FC values obtained from the *M. abscessus* transcriptomes in Mϕ and the *M. chelonae*
188 transcriptome in Ac (**Sup. Figure 3**). This comparison highlighted 45 *M. abscessus* genes (**Sup.**
189 **Table 2**). We also listed the most induced genes in Mϕ (38 genes) (**Sup. Table 3**). From the
190 comparison with the Ac transcriptomes, we constructed deletion mutants in 6 loci (ΔOP1 to
191 ΔOP6) (**Table 3**). From the *M. abscessus* transcriptome in Mϕ we constructed deletion mutants
192 in 5 loci (ΔOP 7 to ΔOP11) among the most induced genes or in genes implicated in the
193 adaptation to intracellular stress (**Table 3**).
194 ΔOP1 to ΔOP6 strains were evaluated for their intracellular multiplication in Ac and in Mϕ
195 (**Figure 5A**). All mutants were attenuated in Ac and Mϕ, except one (ΔOP5), which multiplied
196 more than the wild-type (wt) strain in Mϕ (**Figure 5A**). All mutated strains had similar growth
197 *in vitro* to the wild type strain (**Sup. Figure 4A**). ΔOP2, 3, 4 and 6 were complemented and all
198 strains recovered the wt phenotype except for the OP4 gene *MAB_2650* potentially encoding
199 an MmpL (**Sup. Figure 4B**).
200 These experiments confirmed the importance of these highly induced genes in Ac, in the intra-
201 Mϕ survival of *M. abscessus*. Several genes (OP2 and 6) are absent from *M. chelonae*, or
202 present in the *M. chelonae* genome but at least four times less induced (OP3 and OP4) in Ac.
203 We have analyzed their contribution towards intracellular survival by overexpressing
204 *M. abscessus* OP2, 3, 6 and *MAB_2649* genes in *M. chelonae* (**Figure 5B, left panel**), which is
205 unable to survive in Mϕ (Sousa et al., 2015). Only the overexpression of *M. abscessus* OP3 and
206 OP4 (*MAB_2649*) increased *M. chelonae* survival in Mϕ (**Figure 5B, right panel**). By
207 comparison, no increase in *M. chelonae* intracellular survival was observed when
208 overexpressing OP2 and OP6 (**Figure 5B, right panel**).
209
210 M. abscessus *highly-induced genes in Mϕ*

The observed defect in intracellular survival was noticed for all mutants from OP7 to OP11 (**Figure 5A**), the ΔOP11 mutant was particularly attenuated (GI<0.1). OP11 (*MAB_4532c*) KO strain tended to be eliminated by Mϕ while the KO growth was similar to the WT growth *in vitro* (**Sup. Figure 4**). When complementing ΔOP11 strain with *MAB_4532c*, we restored the wt phenotype (**Figure 6A**). *MAB_4532c* encodes an Eis N-acetyl transferase protein, according to a motif analysis (InterProScan 5). Of interest, *M. abscessus* contains two *eis* genes, named $eis1_{MAB}$ (*MAB_4124*) and $eis2_{MAB}$ (*MAB_4532c*) while *M. tuberculosis* possesses a single eis_{MTB} gene (*Rv2416c*), $eis1_{MAB}$ (*MAB_4124*) being the closest homolog by Bidirectional Best Hit (BBH) search. No conservation of synteny was observed between the respective genomic regions in *M. abscessus* and *M. tuberculosis* (**Sup. Figure 5A**). In contrast, the $eis2_{MAB}$ locus shows some similarity and conservation with the *M. tuberculosis mmpL11* locus, with inverted and syntenic conservation of groups of genes (**Sup. Figure 5B**). The eis_{MTB} locus was well-conserved in *M. abscessus* and corresponds to *MAB_1619-MAB_1627* and *MAB_1633-MAB_1637* regions (**Sup. Figure 5C**). Both $eis1_{MAB}$ and $eis2_{MAB}$ were found close to *mmpL* (brown arrows) and/or *mmpS* (orange arrow) genes (**Sup. Figure 5**). In the *M. abscessus eis2* locus, an *mmpL* gene (*MAB_4529*) was conserved in *M. tuberculosis* corresponding to *mmpL11* (**Sup. Figure 5B**). To assess the function of *M. abscessus eis* genes we performed transcomplementation of KO strains (Δ$eis1_{MAB}$ and Δ$eis2_{MAB}$) with *M. tuberculosis eis* (eis_{MTB}). Of interest, and unlike $eis2_{MAB}$, $eis1_{MAB}$ was suppressed inside Mϕ (**Sup. Figure 6**) and less impaired in its intracellular survival (**Figures 6A-B**). Complementation of Δ$eis1_{MAB}$ and Δ$eis2_{MAB}$ with $eis1_{MAB}$ or $eis2_{MAB}$ respectively allowed the recovery of the intracellular survival for both mutants (**Figures 6A-B**). However, complementation of both mutants with the eis_{MTB} gene allowed only partial restoration of the intracellular replicative phenotype for the Δ$eis2_{MAB}$ mutant, but no restoration was observed for Δ$eis1_{MAB}$ mutant (**Figure 6A-B**). Similar behaviors regarding apoptosis, necrosis, autophagy and phagosomal acidification were observed when

236 comparing the wt *M. abscessus* strain with the Δ*eis2*$_{MAB}$ mutant (**Sup. Figure 7**). However, two
237 major differences were observed. First, infection of Mϕ with the Δ*eis2*$_{MAB}$ strain (at a MOI of
238 50) was associated with higher production of ROS by the cells and loss of *eis2*$_{MAB}$ also
239 sensitized *M. abscessus* to ROS and notably to H_2O_2 (**Figures 6C-D**). Secondly, the Δ*eis2*$_{MAB}$
240 mutant was unable to damage the phagosomal membrane and to provoke phagosome-cytosol
241 contact as compared to the wt and complemented *M. abscessus* strains (**Figure 6E**).
242

Discussion

The main objective of this work was to understand the genetic and molecular basis for the ability of *M. abscessus* to withstand and survive in eukaryotic phagocytic cells. Identification of genes strongly induced after infection of Ac allowed us to reveal those genes that play key roles in Mϕ intracellular survival. Conversely, identification of genes strongly induced after infection of Mϕ allowed us to reveal those essential to Ac intracellular survival with the exception of one mutant, OP5 (*MAB_4663*) encoding a protein of unknown function, that showed enhanced growth in Mϕ. KO mutants constructed on the basis of the results from transcriptomic analyses allowed the identification of genes required for bacterial survival in phagocytes. These results are complementary to a previous *Tn M. abscessus* library viability screen in Ac, permitting the identification of two other intracellular virulence factors, namely the type VII secretion system ESX4 and the lipid transport protein $MmpL8_{MAB}$ (Dubois et al., 2018b; Laencina et al., 2018). The intracellular defects of strains that were deleted for genes highly induced in amoeba (induced at least four times more compared to the intramacrophagic transcriptome of *M. abscessus* and to the intra-amoebal transcriptome of *M. chelonae* (OP1 to OP6)), suggest that the transcriptomic changes observed following a co-culture in amoebae reflected the response of *M. abscessus* in Mϕ. In addition, co-culturing *M. abscessus* in amoebae enhances the virulence of *M. abscessus* even *in vivo* through the induction of the PLC virulence gene (Bakala N'Goma *et al.*, 2015). These transcriptomic analyses highlight that exposure to the amoebal intracellular environment potentiates *M. abscessus* virulence, increasing the resistance of the bacteria for future encounters with phagocytic cells that form part of the innate defense of the host.

Most of the 6 loci (OP1 to OP6) studied encode for hypothetical proteins, with the exception of the *MAB_1517c* gene that encodes a probable O-methyltransferase (OP3), and the *MAB_2649* and *MAB_2650* genes encoding an MmpS and an MmpL, respectively (OP4) (**Table 2**) (Viljoen

et al., 2017). At the *M. abscessus* OP2 locus, that mainly comprises genes of unknown function, we used a motif analysis to identify an ABC transporter, FecCD/TroCD-like in the MAB_1243c protein and an alkaline shock protein Asp23 in the MAB_1247c protein. A motif analysis performed on *M. abscessus* OP6 gene shows that *MAB_4791c* encodes a protein implicated in the twin-arginine translocation pathway (see below). Notably, the over-induction of *MAB_2649* and *MAB_1517c* in *M. chelonae* favors its replication in Mϕ, suggesting that the high induction of these two genes in amoeba may trigger *M. abscessus* virulence.

A striking finding of our work is the essential role of the $eis2_{Mab}$ gene in early resistance to the microbicidal action of Mϕ, via phagosomal membrane damage and cytosol contact, that allows the intracellular survival of *M. abscessus*. Although *M. abscessus* possesses two *Eis* genes, there is no redundancy in their respective functions; the $eis1_{Mab}$ mutant presented a similar behavior to the wt strain in Mϕ, with only the loss of a $\log_{10}$ CFU at 5 dpi, compared to the quasi-total clearance of the $eis2_{Mab}$ mutant in Mϕ. Despite higher genomic identity between $eis1_{MAB}$ and eis_{MTB}, the restoration of the phenotype when complemented with eis_{MTB} was observed only for the $eis2_{MAB}$ mutant, demonstrating the similar role of $eis2_{MAB}$ to what is described for eis_{MTB} in virulence. However the deletion of this gene in *M. abscessus* is more deleterious for the bacterium in Mϕ compared to the deletion of $eis_{MTB,}$ (Wei *et al.*, 2000; Wu *et al.*, 2009). Eis_{MTB} gene has been described as being important for *M. tuberculosis* survival inside Mϕ by controlling host cell apoptosis, autophagy, ROS production and innate immune defenses (Shin et al., 2010). As also observed in *M. tuberculosis* (Shin et al., 2010), increasing the MOI (to 50) revealed further differences between $eis2_{MAB}$ KO and wt strains with regard to resistance to oxidized derivatives; however, this bacterial-load effect has not yet been observed for cell death mechanisms.

One of the peculiarities of the locus $eis2_{MAB}$ is to possess similarities with a genomic region of *M. tuberculosis*, within which is found the gene *mmpL11*. The potential counterpart in

293 *M. abscessus* would be *MAB_4529* (**Sup. Figure 5**). Most of MmpL are lipid transporters
294 implicated in cell physiology and virulence (Chalut, 2016; Viljoen et al., 2017). *M. abscessus*
295 has 27 MmpLs, twice as much as *M. tuberculosis* (Viljoen et al., 2017). In *M. tuberculosis*,
296 MmpL11 is implicated in heme iron acquisition (Owens et al., 2013) and transport of mycolic
297 acid wax ester and long-chain triacylglycerols (Wright et al., 2017). Three genes conserved in
298 the *M. abscessus eis2* locus encode for proteins belonging to lipid transport and metabolism
299 pathways (COG I), which suggests, together with the conservation seen with the *M.*
300 *tuberculosis mmpL11* locus, that the *M. abscessus eis2* locus might also participate in cell wall
301 biogenesis (Yamaryo-Botte et al., 2015).
302 Transcriptomic analysis revealed that nine *M. abscessus* genes, whose orthologues in
303 *M. tuberculosis* contribute to virulence, were highly induced during infection of Mϕ (**Sup.**
304 **Table 2**). Among their gene products, WhiB7 and DevR-DevS are implicated in stress sensing
305 (Kumar et al., 2011). WhiB7, a Fe-S cluster protein, was shown to be induced in response to
306 perturbation in amino-acid metabolism, under reducing intracellular state, iron depletion and
307 increased temperatures (Geiman et al., 2006). The 20-fold increase of *M. abscessus whiB7* in
308 Mϕ suggests that *M. abscessus* may undergo similar stresses in Mϕ. The DevR response
309 regulator of the histidine kinase DevS was also highly up-regulated. In *M. tuberculosis*, the
310 *devR-devS* two-component system (also known as the DosR system) is activated in response to
311 hypoxia (Sherman et al., 2001). Likewise, *M. abscessus MAB_2562c,* the orthologue of
312 *Rv0081,* was induced 10-fold in Mϕ. A putative orthologue (*MAB_1409c*) of the dormancy
313 response gene *Rv1258c* was also strongly induced in intra-macrophagic *M. abscessu*s. The
314 conserved alpha-ketoglutarate-dependent dioxygenase AlkB-encoding gene is thought to be
315 involved in fatty acid metabolism, or in protection against DNA methylation. The *aspC* gene
316 was induced 8-fold; AspC mediates nitrogen transfer from aspartate to glutamate, which in turn,
317 together with glutamine, provides nitrogen to most of the biosynthesis pathways. This is thought

to be essential in *M. tuberculosis* (Sassetti et al., 2003), while aspartate is required for mycobacterial virulence (Gouzy et al., 2013). *M. abscessus katA* gene, which is conserved in *M. avium* and *Listeria monocytogenes*, is a catalase that degrades H_2O_2 into water and oxygen in a single reaction. Such a reaction, enabling resistance to oxidative metabolites, may be an important mechanism of bacillary survival within the host phagocyte (Manca et al., 1999). *M. abscessus eamA (MAB_0677c)*, which is thought to encode a drug/metabolite transporter, was induced in Mϕ. Two additional genes (*MAB_3762* and *MAB*_3180) encoding proteins with an EamA domain were also highly induced. Finally, at the molecular function level, it appears that six of the most highly induced genes in *M. abscessus* in Mϕ encode acyl or N-acetyl transferase proteins playing a role in post-translational modifications.

The *M. abscessus* transcriptomes' comparison in Ac or Mϕ allowed differences in metabolic adaptations to be highlighted. In Mϕ, *M. abscessus* enters a slow replicative stage, and activates the detoxification and protein secretion pathways. By comparison, in amoebae *M. abscessus* switches on protein synthesis, lipid transport and metabolism, transcription of genes involved in post-translational modifications (PTM), protein turnover and chaperones (COG O), reflecting a more active and replicative behavior as compared to a more persistent state in Mϕ. Actually, cell wall biogenesis including peptidoglycan and glycosaminoglycan biosynthetic processes were down-regulated in Mϕ. Similarly, *mtrA*, *phoP* and *devR* were differently regulated, with only *devR* up-regulated in Mϕ, confirming the switch towards a slow growth stage for *M. abscessus* in Mϕ.

Over-representation of the COG O (post-translational modification, protein turnover, molecular chaperone) category in *M. abscessus* infecting Ac indicates that *M. abscessus* may alter cellular processes during its interactions with host cells via PTM, as described in various pathogens (Ribet and Cossart, 2010; Müller *et al.*, 2010; Parra *et al.*, 2017). Protein turnover does not only help in clearing of old proteins but also aids a fast adaptation to nutrient poor environments

(Goldberg and St. John, 1976). Molecular chaperones help pathogens override unfavorable conditions found in the host such as heat shock, oxidative and acid stresses (Neckers and Tatu, 2008). They also contribute to the inhibition of lysosomal fusion and favor bacterial growth (Neckers and Tatu, 2008). Molecular chaperones may therefore form a first line of defense and help consolidate pathogen virulence. Thus, over-representation of the COG O inside amoebae might reflect specific intracellular cues the mycobacterium faced from the early time points post infection.

In Ac, the most enriched GO is adenine salvage (GO:0006168) (**Figure 2**). This GO represents any process that generates adenine from derivatives without any *de novo* synthesis. Mycobacteria are able to limit the synthesis of this high energy demanding nucleotide (Ducati et al., 2011). Mycobacteria are also capable of scavenging free nitrogenous bases from the medium (Ducati et al., 2011). Under conditions of low energy availability or rapid multiplication, the salvage pathway may then be the main source of maintaining the nucleotide pool (Ducati et al., 2011).

Sulfur metabolism (GO:0000103), hydrogen sulfide (H_2S) biosynthetic pathway (GO:0070814) and detoxification via Fe-S cluster assembly proteins (GO:0016226) in addition to polyamine transport (GO:0015846), were also enriched by *M. abscessus* in Ac. In its reduced form, sulfur is used in the biosynthesis of the amino acid cysteine that is one of the prime targets for reactive nitrogen intermediates (Rhee et al., 2005). Those pathways might play a key role in *M. abscessus* survival in phagocytic cells, since genes involved in the metabolism of sulfur have consistently been identified as up-regulated in conditions that mimic the intra-macrophagic environment and during Mϕ infection for *M. tuberculosis* (Schnappinger *et al.*, 2003). As for polyamines (cadaverine, putrescine and spermidine), they are known to have pleiotropic effects on cells via: their interaction with nucleic acids; a role in bacterial virulence

by allowing mycobacterial escape from the phagolysosome; toxin activity or protection from oxidative and acid stress has also been demonstrated (Shah and Swiatlo, 2008).

In Mϕ, glycerol ether metabolic process, MEP pathway and L-proline biosynthetic processes were the most enriched. Glycerol ether metabolic process corresponds to glycerophospholipids-seminolipids-plasmecholine metabolism and cellular amide biosynthetic processes. The MEP pathway is required for isoprenoid precursor biosynthesis (Rohmer et al., 1993). A wide variety of monoterpenes and diterpenes belong to isoprenoid classes which function as toxins, growth inhibitors, or other secondary metabolites (Gershenzon and Dudareva, 2007). Finally, proline has been reported as an important factor in the adaptation of mycobacteria to slow growth rate and hypoxia (Berney *et al.*, 2012). It is believed that the proline-utilization pathway protects mycobacterial cells by detoxifying methylglyoxal, a by-product of endogenous glycerol metabolism (Berney *et al.*, 2012) that can damage DNA and proteins within cells. Up-regulation of base-excision repair suggests that intracellular mycobacteria undergo DNA damage. Protein folding was also enriched, as well as the type II secretion system, which was enriched by more than two-fold. This secretion system promotes the specific transport of folded periplasmic proteins across a dedicated channel in the outer membrane, and it facilitates both Sec and Tat pathways to secrete proteins into the periplasm. Potential roles for SecA1 and SecA2 in *M. tuberculosis* dormancy has been reported while the Tat pathway was shown to contribute to virulence in *Legionella pneumophila* for instance, by aiding secretion of Phospholipase C (Rossier and Cianciotto, 2005), a virulence factor conserved in *M. abscessus* (Ripoll *et al.*, 2009).

Both Ac and Mϕ were sensed as a stressful environment by *M. abscessus,* evidenced by the up-regulation of genes known to be involved in multiple stress responses. Induction of low O_2 and low NO response genes confirm that hypoxic environments are encountered by *M. abscessus* both in Ac and Mϕ.

In conclusion, our findings confirm that the amoeba-induced genes play a role in potentiating the subsequent survival of *M. abscessus* in Mϕ. Both environments have commonalities, in terms of metabolic switches, especially to withstand the host response. It is through this preparation during its intra-amoebic life that *M. abscessus* is able to withstand the noxious Mϕ environment, especially thanks to several genes whose role has been confirmed during this work. The multiple leads opened during this work must now be followed to complete this viewpoint of synergistic potentiation of virulence conferred by the amoeba to *M. abscessus*, including the ultimate mechanisms of manipulation of the host's defense systems as seen with other intracellular pathogens.

REFERENCES

Adékambi T, Ben Salah S, Khlif M, Raoult D, Drancourt M. 2006. Survival of environmental mycobacteria in Acanthamoeba polyphaga. *Appl Environ Microbiol* **72**:5974–5981. doi:10.1128/AEM.03075-05

Ahmed N, Saini V, Raghuvanshi S, Khurana JP, Tyagi AK, Tyagi AK, Hasnain SE. 2007. Molecular Analysis of a Leprosy Immunotherapeutic Bacillus Provides Insights into Mycobacterium Evolution. *PLoS One* **2**:e968. doi:10.1371/journal.pone.0000968

Angenent LT, Kelley ST, St Amand A, Pace NR, Hernandez MT. 2005. Molecular identification of potential pathogens in water and air of a hospital therapy pool. *Proc Natl Acad Sci U S A* **102**:4860–5. doi:10.1073/pnas.0501235102

Bakala N'Goma JC, Le Moigne V, Soismier N, Laencina L, Le Chevalier F, Roux A-L, Poncin I, Serveau-Avesque C, Rottman M, Gaillard J-L, Etienne G, Brosch R, Herrmann J-L, Canaan S, Girard-Misguich F. 2015. Mycobacterium abscessus phospholipase C expression is induced during coculture within amoebae and enhances M. abscessus virulence in mice. *Infect Immun* **83**:780–791. doi:10.1128/IAI.02032-14

Barker J, Brown MRW. 1994. Trojan Horses of the microbial world: protozoa and the survival of bacterial pathogens in the environment. *Microbiology* **140**:1253–1259. doi:10.1099/00221287-140-6-1253

Ben Salah I, Adékambi T, Drancourt M. 2009. Mycobacterium phocaicum in therapy pool water. *Int J Hyg Environ Health* **212**:439–444. doi:10.1016/j.ijheh.2008.10.002

Benjamini, Hochberg. 1995. Controlling the False Discovery Rate: A Practical and Powerful Approach to Multiple Testing. *J R Stat Soc Ser B* **57**:289–300.

Berney M, Weimar MR, Heikal A, Cook GM. 2012a. Regulation of proline metabolism in mycobacteria and its role in carbon metabolism under hypoxia. *Mol Microbiol* **84**:664–81. doi:10.1111/j.1365-2958.2012.08053.x

Berney M, Weimar MR, Heikal A, Cook GM. 2012b. Regulation of proline metabolism in mycobacteria and its role in carbon metabolism under hypoxia. *Mol Microbiol* **84**:664–681. doi:10.1111/j.1365-2958.2012.08053.x

Chalut C. 2016. MmpL transporter-mediated export of cell-wall associated lipids and siderophores in mycobacteria. *Tuberculosis (Edinb)* **100**:32–45. doi:10.1016/j.tube.2016.06.004

Cirillo JD, Falkow S, Tompkins LS, Bermudez LE. 1997. Interaction of Mycobacterium avium with environmental amoebae enhances virulence. *Infect Immun* **65**:3759–67.

Dubois V, Laencina L, Bories A, Le Moigne V, Pawlik A, Herrmann J-L, Girard-Misguich F. 2018a. Identification of Virulence Markers of Mycobacterium abscessus for Intracellular Replication in Phagocytes. *J Vis Exp*. doi:10.3791/57766

Dubois V, Viljoen A, Laencina L, Le Moigne V, Bernut A, Dubar F, Blaise M, Gaillard J-L, Guérardel Y, Kremer L, Herrmann J-L, Girard-Misguich F. 2018b. MmpL8MAB controls Mycobacterium abscessus virulence and production of a previously unknown glycolipid family. *Proc Natl Acad Sci U S A* 201812984. doi:10.1073/pnas.1812984115

Ducati RG, Breda A, Basso LA, Santos DS. 2011. Purine Salvage Pathway in Mycobacterium tuberculosis. *Curr Med Chem* **18**:1258–75.

Eddyani M, De Jonckheere JF, Durnez L, Suykerbuyk P, Leirs H, Portaels F. 2008. Occurrence of free-living amoebae in communities of low and high endemicity for Buruli ulcer in southern Benin. *Appl Environ Microbiol* **74**:6547–53. doi:10.1128/AEM.01066-08

447 Falkinham JO. 2009. Surrounded by mycobacteria: nontuberculous mycobacteria in the
448 human environment. *J Appl Microbiol* **107**:356–67. doi:10.1111/j.1365-
449 2672.2009.04161.x
450 Geiman DE, Raghunand TR, Agarwal N, Bishai WR. 2006. Differential Gene Expression in
451 Response to Exposure to Antimycobacterial Agents and Other Stress Conditions among
452 Seven Mycobacterium tuberculosis whiB-Like Genes. *Antimicrob Agents Chemother*
453 **50**:2836–2841. doi:10.1128/AAC.00295-06
454 Gershenzon J, Dudareva N. 2007. The function of terpene natural products in the natural
455 world. *Nat Chem Biol* **3**:408–414. doi:10.1038/nchembio.2007.5
456 Goldberg AL, St. John AC. 1976. Intracellular Protein Degradation in Mammalian and
457 Bacterial Cells: Part 2. *Annu Rev Biochem* **45**:747–804.
458 doi:10.1146/annurev.bi.45.070176.003531
459 Gomila M, Ramirez A, Gasco J, Lalucat J. 2008. Mycobacterium llatzerense sp. nov., a
460 facultatively autotrophic, hydrogen-oxidizing bacterium isolated from haemodialysis
461 water. *Int J Syst Evol Microbiol* **58**:2769–2773. doi:10.1099/ijs.0.65857-0
462 Gouzy A, Poquet Y, Neyrolles O. 2013. A central role for aspartate in Mycobacterium
463 tuberculosis physiology and virulence. *Front Cell Infect Microbiol* **3**:68.
464 doi:10.3389/fcimb.2013.00068
465 Greub G, Raoult D. 2004. Microorganisms resistant to free-living amoebae. *Clin Microbiol*
466 *Rev* **17**:413–33.
467 Griffith DE, Aksamit T, Brown-Elliott B a, Catanzaro A, Daley C, Gordin F, Holland SM,
468 Horsburgh R, Huitt G, Iademarco MF, Iseman M, Olivier K, Ruoss S, von Reyn CF,
469 Wallace RJ, Winthrop K. 2007. An official ATS/IDSA statement: diagnosis, treatment,

and prevention of nontuberculous mycobacterial diseases. *Am J Respir Crit Care Med* **175**:367–416. doi:10.1164/rccm.200604-571ST

Guidotti TL, Ragain L, de Haas P, van Soolingen D. 2008. Communicating with healthcare providers. *J Water Health* **6**:s53. doi:10.2166/wh.2008.032

Gutierrez MC, Brisse S, Brosch R, Fabre M, Omaïs B, Marmiesse M, Supply P, Vincent V. 2005. Ancient Origin and Gene Mosaicism of the Progenitor of Mycobacterium tuberculosis. *PLoS Pathog* **1**:e5. doi:10.1371/journal.ppat.0010005

Hartman T, Weinrick B, Vilchèze C, Berney M, Tufariello J, Cook GM, Jacobs WR, Jr. 2014. Succinate dehydrogenase is the regulator of respiration in Mycobacterium tuberculosis. *PLoS Pathog* **10**:e1004510. doi:10.1371/journal.ppat.1004510

Jamet S, Quentin Y, Coudray C, Texier P, Laval F, Daffé M, Fichant G, Cam K. 2015. Evolution of Mycolic Acid Biosynthesis Genes and Their Regulation during Starvation in Mycobacterium tuberculosis. *J Bacteriol* **197**:3797–811. doi:10.1128/JB.00433-15

Kumar A, Farhana A, Guidry L, Saini V, Hondalus M, Steyn AJC. 2011. Redox homeostasis in mycobacteria: the key to tuberculosis control? *Expert Rev Mol Med* **13**:e39. doi:10.1017/S1462399411002079

Laencina L, Dubois V, Le Moigne V, Viljoen A, Majlessi L, Pritchard J, Bernut A, Piel L, Roux A-L, Gaillard J-L, Lombard B, Loew D, Rubin EJ, Brosch R, Kremer L, Herrmann J-L, Girard-Misguich F. 2018. Identification of genes required for Mycobacterium abscessus growth in vivo with a prominent role of the ESX-4 locus. *Proc Natl Acad Sci* **115**:E1002–E1011. doi:10.1073/pnas.1713195115

Lamrabet O, Medie FM, Drancourt M. 2012. Acanthamoeba polyphaga-enhanced growth of mycobacterium smegmatis. *PLoS One* **7**. doi:10.1371/journal.pone.0029833

493 Lavania M, Katoch K, Katoch VM, Gupta AK, Chauhan DS, Sharma R, Gandhi R, Chauhan V,
494 Bansal G, Sachan P, Sachan S, Yadav VS, Jadhav R. 2008. Detection of viable
495 Mycobacterium leprae in soil samples: Insights into possible sources of transmission of
496 leprosy. *Infect Genet Evol* **8**:627–631. doi:10.1016/j.meegid.2008.05.007
497 Le Moigne V, Belon C, Goulard C, Accard G, Bernut A, Pitard B, Gaillard J-L, Kremer L,
498 Herrmann J-L, Blanc-Potard A-B. 2016. MgtC as a Host-Induced Factor and Vaccine
499 Candidate against Mycobacterium abscessus Infection. *Infect Immun* **84**:2895–2903.
500 doi:10.1128/IAI.00359-16
501 Love MI, Huber W, Anders S. 2014. Moderated estimation of fold change and dispersion for
502 RNA-seq data with DESeq2. *Genome Biol* **15**:550. doi:10.1186/s13059-014-0550-8
503 Manca C, Paul S, Barry CE, Freedman VH, Kaplan G, Kaplan G. 1999. Mycobacterium
504 tuberculosis catalase and peroxidase activities and resistance to oxidative killing in
505 human monocytes in vitro. *Infect Immun* **67**:74–9.
506 Medjahed H, Singh AK. 2010. Genetic manipulation of Mycobacterium abscessus. *Curr Protoc*
507 *Microbiol* **Chapter 10**:Unit 10D.2. doi:10.1002/9780471729259.mc10d02s18
508 Mukhopadhyay S, Nair S, Ghosh S. 2012. Pathogenesis in tuberculosis: transcriptomic
509 approaches to unraveling virulence mechanisms and finding new drug targets. *FEMS*
510 *Microbiol Rev* **36**:463–485. doi:10.1111/j.1574-6976.2011.00302.x
511 Müller MP, Peters H, Blümer J, Blankenfeldt W, Goody RS, Itzen A. 2010. The Legionella
512 effector protein DrrA AMPylates the membrane traffic regulator Rab1b. *Science*
513 **329**:946–9. doi:10.1126/science.1192276
514 Neckers L, Tatu U. 2008. Molecular chaperones in pathogen virulence: emerging new targets
515 for therapy. *Cell Host Microbe* **4**:519–27. doi:10.1016/j.chom.2008.10.011

516 Owens CP, Chim N, Graves AB, Harmston CA, Iniguez A, Contreras H, Liptak MD, Goulding
517 CW. 2013. The mycobacterium tuberculosis secreted protein Rv0203 transfers heme to
518 membrane proteins MmpL3 and MmpL11. *J Biol Chem* **288**:21714–21728.
519 doi:10.1074/jbc.M113.453076
520 Pagnier I, Raoult D, La Scola B. 2008. Isolation and identification of amoeba-resisting bacteria
521 from water in human environment by using an Acanthamoeba polyphaga co-culture
522 procedure. *Environ Microbiol* **10**:1135–1144. doi:10.1111/j.1462-2920.2007.01530.x
523 Parra J, Marcoux J, Poncin I, Canaan S, Herrmann JL, Nigou J, Burlet-Schiltz O, Rivière M.
524 2017. Scrutiny of Mycobacterium tuberculosis 19 kDa antigen proteoforms provides
525 new insights in the lipoglycoprotein biogenesis paradigm. *Sci Rep* **7**:43682.
526 doi:10.1038/srep43682
527 Rhee KY, Erdjument-Bromage H, Tempst P, Nathan CF. 2005. S-nitroso proteome of
528 Mycobacterium tuberculosis: Enzymes of intermediary metabolism and antioxidant
529 defense. *Proc Natl Acad Sci* **102**:467–472. doi:10.1073/pnas.0406133102
530 Ribet D, Cossart P. 2010. Pathogen-Mediated Posttranslational Modifications: A Re-emerging
531 Field. *Cell* **143**:694–702. doi:10.1016/J.CELL.2010.11.019
532 Ripoll F, Pasek S, Schenowitz C, Dossat C, Barbe V, Rottman M, Macheras E, Heym B,
533 Herrmann J-L, Daffé M, Brosch R, Risler J-L, Gaillard J-L. 2009. Non mycobacterial
534 virulence genes in the genome of the emerging pathogen Mycobacterium abscessus.
535 *PLoS One* **4**:e5660. doi:10.1371/journal.pone.0005660
536 Rohmer M, Knani M, Simonin P, Sutter B, Sahm H. 1993. Isoprenoid biosynthesis in bacteria:
537 a novel pathway for the early steps leading to isopentenyl diphosphate. *Biochem J* **295 (**
538 **Pt 2**:517–24.

539 Rossier O, Cianciotto NP. 2005. The Legionella pneumophila tatB gene facilitates secretion of
540 phospholipase C, growth under iron-limiting conditions, and intracellular infection.
541 *Infect Immun* **73**:2020–32. doi:10.1128/IAI.73.4.2020-2032.2005
542 Roux A-L, Viljoen A, Bah A, Simeone R, Bernut A, Laencina L, Deramaudt T, Rottman M,
543 Gaillard J-LJ-L, Majlessi L, Brosch R, Girard-Misguich F, Vergne I, de Chastellier C, Kremer
544 L, Herrmann J-LJ-L. 2016. The distinct fate of smooth and rough Mycobacterium
545 abscessus variants inside macrophages. *Open Biol* **6**:160185. doi:10.1098/rsob.160185
546 Salah IB, Ghigo E, Drancourt M. 2009. Free-living amoebae, a training field for macrophage
547 resistance of mycobacteria. *Clin Microbiol Infect* **15**:894–905. doi:10.1111/j.1469-
548 0691.2009.03011.x
549 Sassetti CM, Boyd DH, Rubin EJ. 2003. Genes required for mycobacterial growth defined by
550 high density mutagenesis. *Mol Microbiol* **48**:77–84.
551 Schnappinger D, Ehrt S, Voskuil MI, Liu Y, Mangan J a, Monahan IM, Dolganov G, Efron B,
552 Butcher PD, Nathan C, Schoolnik GK. 2003a. Transcriptional Adaptation of
553 Mycobacterium tuberculosis within Macrophages: Insights into the Phagosomal
554 Environment. *J Exp Med* **198**:693–704. doi:10.1084/jem.20030846
555 Schnappinger D, Ehrt S, Voskuil MI, Liu Y, Mangan JA, Monahan IM, Dolganov G, Efron B,
556 Butcher PD, Nathan C, Schoolnik GK. 2003b. Transcriptional Adaptation of
557 *Mycobacterium tuberculosis* within Macrophages. *J Exp Med* **198**:693–704.
558 doi:10.1084/jem.20030846
559 Shah P, Swiatlo E. 2008. MicroReview A multifaceted role for polyamines in bacterial
560 pathogens. doi:10.1111/j.1365-2958.2008.06126.x
561 Sherman DR, Mdluli K, Hickey MJ, Barry CE, Stover CK. 1999. AhpC, oxidative stress and drug
562 resistance in Mycobacterium tuberculosis. *Biofactors* **10**:211–7.

563 Sherman DR, Voskuil M, Schnappinger D, Liao R, Harrell MI, Schoolnik GK. 2001. Regulation
564 of the Mycobacterium tuberculosis hypoxic response gene encoding alpha -crystallin.
565 *Proc Natl Acad Sci U S A* **98**:7534–9. doi:10.1073/pnas.121172498
566 Shin D-M, Jeon B-Y, Lee H-M, Jin HS, Yuk J-M, Song C-H, Lee S-H, Lee Z-W, Cho S-N, Kim J-M,
567 Friedman RL, Jo E-K. 2010. Mycobacterium tuberculosis Eis Regulates Autophagy,
568 Inflammation, and Cell Death through Redox-dependent Signaling. *PLoS Pathog*
569 **6**:e1001230. doi:10.1371/journal.ppat.1001230
570 Siddiqui R, Khan NA. 2012. Acanthamoeba is an evolutionary ancestor of macrophages: a
571 myth or reality? *Exp Parasitol* **130**:95–7. doi:10.1016/j.exppara.2011.11.005
572 Simeone R, Sayes F, Song O, Gröschel MI, Brodin P, Brosch R, Majlessi L. 2015. Cytosolic
573 access of Mycobacterium tuberculosis: critical impact of phagosomal acidification
574 control and demonstration of occurrence in vivo. *PLoS Pathog* **11**:e1004650.
575 doi:10.1371/journal.ppat.1004650
576 Sousa S, Bandeira M, Carvalho PA, Duarte A, Jordao L. 2015. Nontuberculous mycobacteria
577 pathogenesis and biofilm assembly. *Int J Mycobacteriology* **4**:36–43.
578 doi:10.1016/J.IJMYCO.2014.11.065
579 Stinear TP, Seemann T, Harrison PF, Jenkin GA, Davies JK, Johnson PDR, Abdellah Z,
580 Arrowsmith C, Chillingworth T, Churcher C, Clarke K, Cronin A, Davis P, Goodhead I,
581 Holroyd N, Jagels K, Lord A, Moule S, Mungall K, Norbertczak H, Quail MA,
582 Rabbinowitsch E, Walker D, White B, Whitehead S, Small PLC, Brosch R, Ramakrishnan
583 L, Fischbach MA, Parkhill J, Cole ST. 2008. Insights from the complete genome sequence
584 of Mycobacterium marinum on the evolution of Mycobacterium tuberculosis. *Genome*
585 *Res* **18**:729–741. doi:10.1101/gr.075069.107

586 Tatusov RL, Galperin MY, Natale DA, Koonin E V. 2000. The COG database: a tool for
587 genome-scale analysis of protein functions and evolution. *Nucleic Acids Res* **28**:33–6.
588 Thomas V, Herrera-rimann K, Blanc DS, Greub G. 2006. Biodiversity of Amoebae and
589 Amoeba-Resisting Bacteria in a Hospital Water Network. *Appl Env Microbiol* **72**:2428–
590 2438. doi:10.1128/AEM.72.4.2428
591 Thomas V, McDonnell G. 2007. Relationship between mycobacteria and amoebae: ecological
592 and epidemiological concerns. *Lett Appl Microbiol* **45**:349–57. doi:10.1111/j.1472-
593 765X.2007.02206.x
594 Thomson RM, Carter R, Tolson C, Coulter C, Huygens F, Hargreaves M. 2013. Factors
595 associated with the isolation of Nontuberculous mycobacteria (NTM) from a large
596 municipal water system in Brisbane, Australia. *BMC Microbiol* **13**:89. doi:10.1186/1471-
597 2180-13-89
598 Vallenet D, Engelen S, Mornico D, Cruveiller S, Fleury L, Lajus A, Rouy Z, Roche D, Salvignol G,
599 Scarpelli C, Médigue C. 2009. MicroScope: a platform for microbial genome annotation
600 and comparative genomics. *Database (Oxford)* **2009**:bap021.
601 doi:10.1093/database/bap021
602 Viljoen A, Dubois V, Girard-Misguich F, Blaise M, Herrmann J-L, Kremer L. 2017. The diverse
603 family of MmpL transporters in mycobacteria: from regulation to antimicrobial
604 developments. *Mol Microbiol* **104**. doi:10.1111/mmi.13675
605 White CI, Birtles RJ, Wigley P, Jones PH. 2010. Mycobacterium avium subspecies
606 paratuberculosis in free-living amoebae isolated from fields not used for grazing. *Vet*
607 *Rec* **166**:401–402. doi:10.1136/vr.b4797
608 Wright CC, Hsu FF, Arnett E, Dunaj JL, Davidson PM, Pacheco SA, Harriff MJ, Lewinsohn DM,
609 Schlesinger LS, Purdy GE. 2017. The Mycobacterium tuberculosis MmpL11 Cell Wall

610 Lipid Transporter Is Important for Biofilm Formation, Intracellular Growth, and
611 Nonreplicating Persistence. *Infect Immun* **85**:e00131-17. doi:10.1128/IAI.00131-17
612 Wu S, Barnes PF, Samten B, Pang X, Rodrigue S, Ghanny S, Soteropoulos P, Gaudreau L,
613 Howard ST. 2009. Activation of the eis gene in a W-Beijing strain of Mycobacterium
614 tuberculosis correlates with increased SigA levels and enhanced intracellular growth.
615 *Microbiology* **155**:1272–81. doi:10.1099/mic.0.024638-0
616 Yamaryo-Botte Y, Rainczuk AK, Lea-Smith DJ, Brammananth R, van der Peet PL, Meikle P,
617 Ralton JE, Rupasinghe TWT, Williams SJ, Coppel RL, Crellin PK, McConville MJ. 2015.
618 Acetylation of Trehalose Mycolates Is Required for Efficient MmpL-Mediated
619 Membrane Transport in Corynebacterineae. *ACS Chem Biol* **10**:734–746.
620 doi:10.1021/cb5007689
621
622

623 MATERIALS AND METHODS

624 **Bacterial strains, plasmids and growth conditions**

625 A clinical isolate of *M. abscessus* subspecies *massiliense s*mooth variant (43S) and *M. chelonae*
626 type strain CCUG 47445 were used for the RNAseq experiments. Gene deletions were
627 performed with CIP 104536T type smooth strain of *M. abscessus* subspecies *abscessus*. Both
628 *M. abscessus* CIP strain and *M. chelonae* type strain were used to perform *in vitro* survival and
629 complementation tests while gene deletions were performed with *M. abscessus* CIP 104536T
630 strain. *M. abscessus* and *M. chelonae* strains were routinely grown aerobically at 37 °C and
631 32°C respectively, in Middlebrook 7H9 medium (Sigma-Aldrich) supplemented with 0.2%
632 glycerol, 1% glucose, and 250 mg/L kanamycin (Thermo Fisher Scientific) when necessary,
633 with 25 mg/L zeocin (Thermo Fisher Scientific) for the knockout strains, and with 25 mg/L
634 zeocin plus 250 mg/L hygromycin (Thermo Fisher Scientific) for complemented strains. *A.*
635 *castellanii* (ATCC 30010) was grown at room temperature without CO_2 in peptone yeast extract
636 glucose (PYG) broth for the amplification of the strain. J774.2 cell line was grown and used as
637 described (Le Moigne et al., 2016; Roux et al., 2016).
638
639 **Gene deletion and complementation**
640 Deletion of genes was performed using the recombineering system as described previously
641 (Medjahed and Singh, 2010; Bakala N'Goma *et al.*, 2015). Growth of the KO strains was
642 checked by measuring the optical density of bacterial cultures in 7H9 medium supplemented
643 with glycerol 0.1%. Complementation was performed after amplifying and cloning genes into
644 the integrative plasmid pMVH361 as described (Bakala N'Goma *et al.*, 2015).
645
646 **RNA isolation and RNA sequencing**

Approximately 10^7 cells were infected in 50 mL tubes, with low agitation, without CO_2. Amoebae were infected at 100 MOI at 32°C. Mϕ were infected at 50 MOI at 37°C. Cells were washed 3 times after 1 hour of infection and resuspended in medium supplemented with amikacin 250 µg/mL and incubated for 1 hour to eliminate extracellular bacteria. Three additional washed were performed and cells were resuspended in medium supplemented with amikacin 50 µg/mL for the rest of the infection. Amoebal cells were harvested 4 h and 16 hpi for intracellular *M. abscessus* RNA isolation 4h and 16 hpi and 16hpi for intracellular *M. chelonae* RNA isolation. Mϕ were harvested for intracellular *M. abscessus* RNA isolation 16H post-infection. RNA isolation was performed as described (Dubois et al., 2018a). Briefly, cells were lysed with a cold solution of Guanidium thiocyanate (GTC), N-Lauryl-sarcosine, Sodium citrate +/- Tween 80 plus β-mercaptoethanol. The lysates containing intracellular bacteria were collected, centrifuged and RNA was isolated from the bacterial pellets with TRIzol. The lysates were then transferred into 2 mL screw tubes containing zirconium beads and were conserved at -80°C for at least 1 day to allow inactivation of RNAses and cells dissolution. Bacteria cells were disrupted with a bead beater by performing to round at 6.500 rpm for 25 seconds, followed by one round at 6.500 rpm for 20 seconds. Two hundred µL of chloroforme isoamyl was added and tubes were immediately mixed for 10 seconds. The mixture was centrifugated at 13.000 rpm for 15 minutes at 4°C. The RNA present in the upper phase was transferred to a fresh tube and precipitated by adding 0.8 volume of isopropanol. Tubes were inverted twice to allow precipitation and kept at -20°C for at least 2 hours. The precipitated RNA was then pelleted by centrifugation at 13.000 rpm for 30 min. at 4°C. The pellet was washed with ethanol (70%) and centrifuged at 13.000 rpm for 10 min at 4°C. The washed pellet was air-dried, re-suspended in RNase-free water and stored at -80°C until cDNA library construction.

671 Control RNA was isolated from bacteria cells grown in amoeba or Mϕ co-culture medium
672 (mowat and DMEM supplemented with 10% Fetal Bovine Serum respectively).
673 Biological replicates were prepared to allow statistical comparisons of infected and non-
674 infected samples.
675
676 **RNA treatments prior to library preparation and library preparation**
677 RNA samples were treated with DNases (AMBION) to remove DNA contaminants, purified
678 with the RNA MEGAclear kit (Thermofisher), and depleted of ribosomal RNA with the
679 riboZero kit (Illumina). RNA (total, depleted, purified) is checked on the Bioanalyser system
680 (Agilent) for its quality and integrity. cDNA libraries were prepared with samples displaying a
681 RIN above 7. RNA concentrations were measured using the nanodrop spectrophotometer
682 (Thermo Scientific) and the Qubit fluorometer (Invitrogen). Libraries were prepared with the
683 TruSeq Stranded RNA LT prep kit cDNA synthesis, set A (Illumina) which consists in: (1)
684 RNA fragmentation, (2) 1st strand cDNA synthesis (Reverse transcriptase and random
685 primers), (3) 2d strand cDNA synthesis (removal of the RNA template and synthesis of a new
686 strand with dUTP), (4) no end repair step, (5) adenylation of 3' ends, (6) ligation of adapters
687 and (7) enrichment of DNA fragments. Libraries are checked for concentration and quality on
688 DNA chips with the Bioanalyzer Agilent. More precise and accurate quantification is performed
689 with sensitive fluorescent-based quantitation assays ("Quant-It" assays kit and QuBit
690 fluorometer, Invitrogen).
691
692 **NGS sequencing and data analysis**
693 Sequencing and statistical analysis were performed in the Transcriptome and Epigenome
694 platform (PF2) of Pasteur Institut, Paris, France. The cDNA libraries were sequenced on
695 Illumina HiSeq 2500 system by performing an SRM run (SR: Single Read, PE: Paired-end

Reads, M: multiplexed samples) of 51 cycles with 7 index bases read. The quality of the sequencing was assessed with the external FastQC program (https://www.bioinformatics.babraham.ac.uk/projects/fastqc/). After the trimming of adapter sequences and low-quality reads with cutadapt version 1.11, reads were aligned with RefSeq assemblies, either *M. abscessus* subsp. *massiliense* strain GO06 assembly (GCF_000277775.2) or *M. chelonae* CCUG 47445 assembly (GCF_001632805.1), using the Bowtie software version 0.12.7 (http://bowtie-bio.sourceforge.net/index.shtml) with defaults parameters. Genes were counted using featureCounts 1.4.6-p3 from Subreads package (parameters: -g gene -t ID -s 1). Differential analysis of gene expression was performed using the R software (version 3.3.1) and the Bioconductor packages DESeq2 (version 1.12.3) (Love et al., 2014) using the default parameters and statistical tests for differential expression were performed applying the independent filtering algorithm. A generalized linear model was set in order to test for the differential expression between the biological conditions. For each pairwise comparison, raw *p*-values were adjusted for multiple testing according to the Benjamini and Hochberg (BH) procedure (Benjamini and Hochberg, 1995) and genes with an adjusted *p*-value lower than 0.05 were considered differentially expressed. Equivalent to *M. abscessus* subsp. *abscessus* CIP strain of *M. abscessus* 43S genes and *M. chelonae* genes were determined by Birectionnal Best Hit search using the Opscan software (http://wwwabi.snv.jussieu.fr/public/opscan/). Differentially expressed genes assignment to COGs was performed using the COG automatic Classification from the MicroScope database (Vallenet et al., 2009). The percentage assignments were compared by performing Fisher's exact tests. GOE analyses were performed with the R software topGO package (Bioconductor) (Alexa *et al.* 2018).

Quantitative real-time PCR

720 qRT-PCR were performed with a CFX96 thermal cycler (Bio-Rad). Controls without reverse
721 transcriptase were done on each RNA sample to rule out DNA contamination. The sigA gene
722 was used as an internal control (Bakala N'Goma *et al.*, 2015). Each qRT-PCR was performed
723 with three biological replicates.
724
725 ***In vitro* survival assays**
726 Survival of strains in amoebae and Mϕ were performed as previously described (Dubois et al.,
727 2018b). Survival tests of KO strains were performed in duplicates three times. Confirmation of
728 attenuated phenotypes and complementation tests were performed in triplicates three times.
729
730 ***Phagosome acidification and phagosomal escape FRET assays Phagosome acidification***
731 Phagosome acidification and phagosomal escape FRET assays and phagosomal escape FRET
732 assays were conducted in THP-1 cells as previously described (Roux et al., 2016; Simeone et
733 al., 2015).
734
735 ***Cell death, autophagy and ROS production assays***
736 Macrophage death following infection with *M. abscessus* was assessed with the Dead Cell
737 Apoptosis Kit with Annexin V FITC and PI for flow cytometry (ThermoFischer). Autophagy
738 was assessed with the Premo™ Autophagy Tandem Sensor RFP-GFP-LC3B Kit
739 (ThermoFisher). ROS production by macrophages was measured with the MitoSOX Red kit
740 (ThermoFisher).
741 Infections were performed as previously described (Dubois et al., 2018b), at 50 MOI, except
742 in the ROS production assay for which the cells were infected 15 min only.
743
744 ***Bacterial sensitivity to H_2O_2***

745 Sensitivity to H_2O_2 was assessed by culturing the bacteria in 7H9 medium suuplemented with
746 glycerol 0,1% and H_20_2 3% (Laboratoires Gillbert) (20 µM). CFU tests were performed at
747 different times post-treatment (2h, 4h, 8h) to determine the number of viable bacteria compared
748 to the wt strain (Growth Index).

749 ACKNOWLEDGEMENT

750 We thank B. G. Marshall (Southampton University) and S. Gordon (University College,

751 Dublin) for their careful reading of the manuscript and for giving valuable comments.

752 V.D. was supported by French Cystic Fibrosis Patients Association Vaincre la Mucoviscidose

753 Grant RF20150501377.

754 **Figure legends**

755 **Figure 1: Description of *M. abscessus* transcriptomes in Ac (A) and Mφ (C).** Differentially
756 expressed genes (DEGs) fold change (FC) in *A. castellanii* (Ac) 4 hpi are plotted against DEGs
757 FC 16 hpi (A). DEGs FC in Ac 16 hpi are also plotted against DEGs FC in macrophages (Mφ)
758 16 hpi (C). DEGs from quadrant 2 (Q2) and 4 (Q4) are genes regulated in the same direction
759 whereas DEGs from Q1 and Q3 are genes regulated in opposite direction. Dots on the plot axes
760 are genes regulated in one condition only. Proportions of DEGs in each case are quantified. ***M.***
761 ***abscessus* adaptations to Ac (B) and Mφ (D) unraveled by COG categorization** Highly
762 regulated genes were assigned to COGs. The genome assignation (framed in black) serves as a
763 reference for COG enrichment tests. Fisher's exact tests were performed to compare the
764 transcriptome sets and the genome set of gene assignments to COG. * $p<0.05$. ** $p<0.01$. ***
765 $p<0.001$. **** $p<0.0001$.

766

767 **Figure 2: Gene ontology enrichment analyses applied on *M. abscessus* intracellular**
768 **transcriptomes.**

769 **A**. Up-regulated genes in Ac 16 hpi. **B**. Up-regulated genes in Mφ. **C**. Down-regulated genes
770 in Ac 16 hpi. **D**. Down-regulated genes in Mφ 16 hpi. Gene onthology (GO) enrichment
771 analysis was performed with the topGO R package. Enriched GOs are sorted according to their
772 enrichment factor (EF), corresponding to the ratio of significant DEGs assigned to the GO over
773 expected assigned DEGs to the GO. Enriched GOs are represented by circles which size is
774 proportional to the amount of significant DEGs assigned. Positive statistical tests are given that
775 face each GO. Method giving the smallest *p*-value is underlined.

776

777 **Figure 3: Intracellular *M. abscessus* relies on fatty acid and cholesterol catabolism.**

778 DEGs FC of genes implicated in Central Carbon Metabolism (CCM) is represented on a Heat
779 Map ranging from blue (DOWN DEGs) to red (UP DEGs). On this Heat Map both *M. abscessus*
780 intra-amoebal (Ac) and intra-macrophagic (Mφ) DEGs are depicted.
781
782 **Figure 4: Regulation of genes required for pathogenic mycobacteria survival *in vitro*.**
783 Regulation of *M. abscessus* genes conserved in *M.* tuberculosis, known to be induced and to
784 contribute to cellular microbicidal defenses of the tubercle bacillus in Mϕ (Mukhopadhyay et
785 al., 2012) is represented on a Heat Map in a blue (repressed genes) to red (induced genes) color
786 scale. On this Heat Map both *M. abscessus* intra-amoebal (Ac) and intra-macrophagic (Mφ)
787 DEGs are depicted and divided in categories: « broad transcription regulators » and genes
788 implicated in the response to various intracellular stress (« Multiple stress response », « Heat
789 Shock response », « Molecular chaperones », « DNA damage repair enzymes », « Response to
790 low O_2 / NO », « Low iron response », « Response to oxidative stress »).
791
792 **Figure 5: Comparative transcriptomic analyses allow identifying genes required for**
793 ***M. abscessus* survival in amoebae and macrophages.**
794 **A**. Intracellular survival of selected KO (ΔOP) in *A. castellani* (Ac) and macrophages (Mφ). **B**.
795 Over-expression of 4 *M. abscessus* virulence genes (left panel) in *M. chelonae* and impacts on
796 *M. chelonae* replication in macrophages (right panel). FC values from *M. chelonae*
797 transcriptome in Ac 16 hpi are compared to FC value mid-log phase cultures of *M. chelonae*
798 strains overexpressing *M. abscessus* genes (left panel). Cells were infected at 10 MOI and
799 colony forming units (CFU) tests were performed 0 and 3 dpi. The relative growth of each strain
800 as compared to *M. abscessus* wt (Growth Index, GI) is given. All experiments were repeated
801 twice or more, in duplicates (A.) or triplicates (B). Statistical analyses were performed with
802 GraphPad PRISM6. Histograms with error bars represent means ± SD. Differences between

803 means were analyzed by ANOVA and the Tukey post-test allowing multiple comparisons to be
804 performed. ns = non-significant. * $p<0.05$. ** $p<0.01$. *** $p<0.001$. **** $p<0.0001$.
805
806 **Figure 6: *M. abscessus eis2* gene is essential for survival in macrophages and shares**
807 **functions with *M. tuberculosis eis* conversely to *M. abscessus eis1*.**
808 **A**. Intracellular survival of *M. abscessus eis2* KO strain ($\Delta eis2_{MAB}$) and complementation in
809 macrophages (Mφ). **B**. Intracellular survival of *M. abscessus eis1* KO strain ($\Delta eis1_{MAB}$) and
810 complementation in Mφ. Macrophages were infected at 10 MOI and colony forming unit (CFU)
811 tests were performed at several times post-infection (0, 1, 3 and 5 dpi). **C.** Control of ROS
812 production by *M. abscessus* Eis2. ROS production by Mφ was assessed by flow cytometry with
813 the Mitosox Red kit, 15 min post-infection at 50 MOI. **D.** Sensitivity of *M. abscessus eis2* KO
814 strain to hydrogen peroxide (H_2O_2). Sensitivity to H_2O_2 was assessed by incubated bacterial
815 cultures with H_2O_2 20 µM during 8 h. The amount of survival cells was determined by
816 performing CFU tests at several hours post-infection (2, 4, 8 hpi). **E.** *Control of phagosomal*
817 *rupture by M. abscessus Eis2.* Phagosomal rupture was assessed by performing a Fluorescence
818 energy transfer (FRET) analysis as previously described (Simeone *et al.*, 2015). Results are
819 depicted as signal overlays per group with 1,000,000 events per condition acquired in not
820 infected cells (NI cells), Heat killed *M. abscessus* (HK), wild-type *M. abscessus* (Mabs wt), KO
821 strains ($\Delta eis2_{MAB}$), KO strains complemented with $eis2_{MAB}$ ($C.eis2_{MAB}$). All experiments were
822 repeated twice or more in triplicates. Statistical analyses were performed with GraphPad
823 PRISM6. Histograms with error bars represent means ± SD. Differences between means were
824 analyzed by ANOVA and the Tukey post-test allowing multiple comparisons to be performed.
825 ns = non-significant. * $p<0.05$. ** $p<0.01$. *** $p<0.001$. **** $p<0.0001$.
826

Figure 1

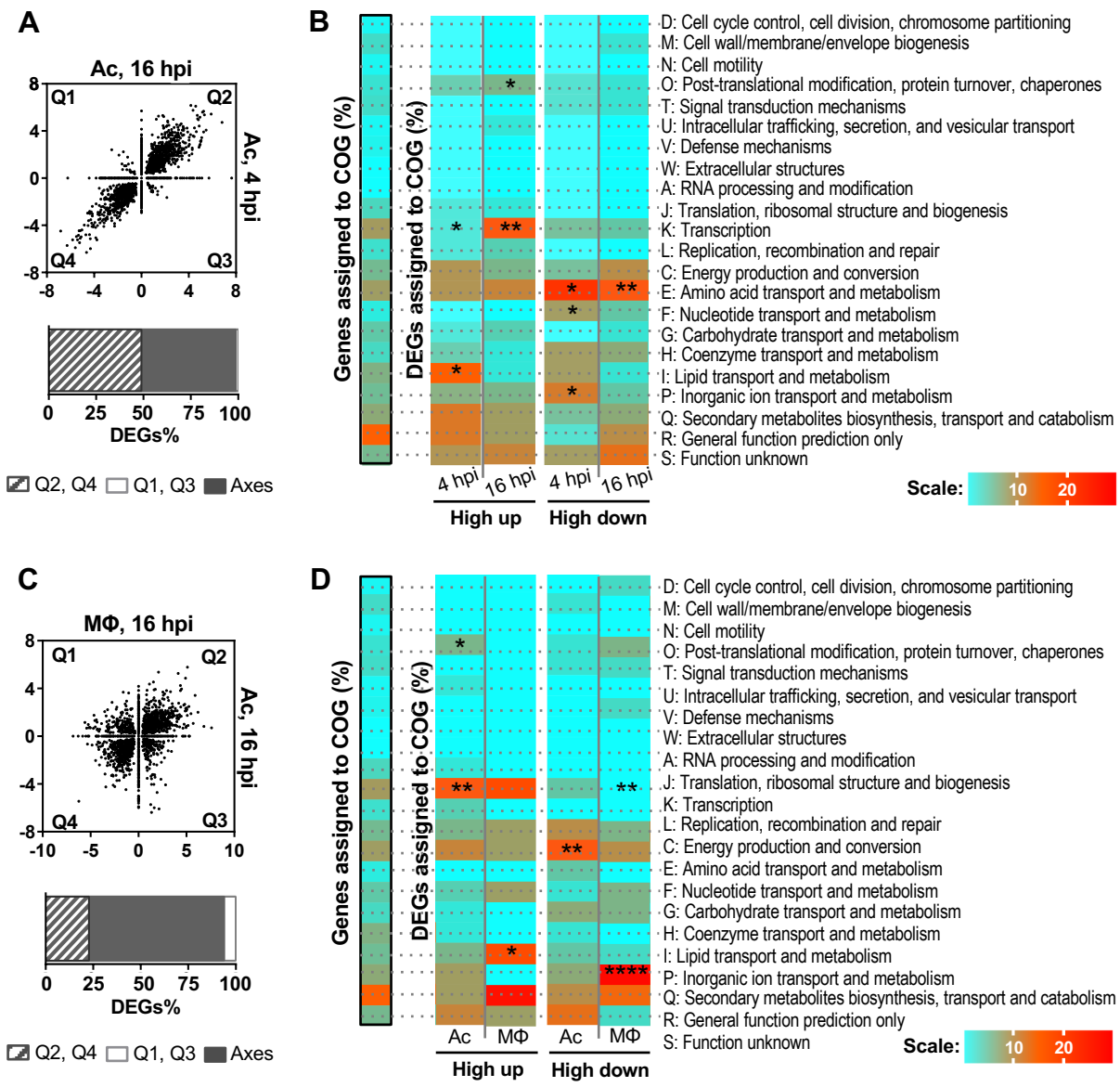
A
Ac, 16 hpi
Q1
Q2
Q3
Q4
Ac, 4 hpi
DEGs%
Q2, Q4
Q1, Q3
Axes
B
Genes assigned to COG (%)
DEGs assigned to COG (%)
4 hpi
16 hpi
High up
High down
D: Cell cycle control, cell division, chromosome partitioning
M: Cell wall/membrane/envelope biogenesis
N: Cell motility
O: Post-translational modification, protein turnover, chaperones
T: Signal transduction mechanisms
U: Intracellular trafficking, secretion, and vesicular transport
V: Defense mechanisms
W: Extracellular structures
A: RNA processing and modification
J: Translation, ribosomal structure and biogenesis
K: Transcription
L: Replication, recombination and repair
C: Energy production and conversion
E: Amino acid transport and metabolism
F: Nucleotide transport and metabolism
G: Carbohydrate transport and metabolism
H: Coenzyme transport and metabolism
I: Lipid transport and metabolism
P: Inorganic ion transport and metabolism
Q: Secondary metabolites biosynthesis, transport and catabolism
R: General function prediction only
S: Function unknown
Scale:
10
20
C
MΦ, 16 hpi
Ac, 16 hpi
D
Ac
MΦ

Figure 2

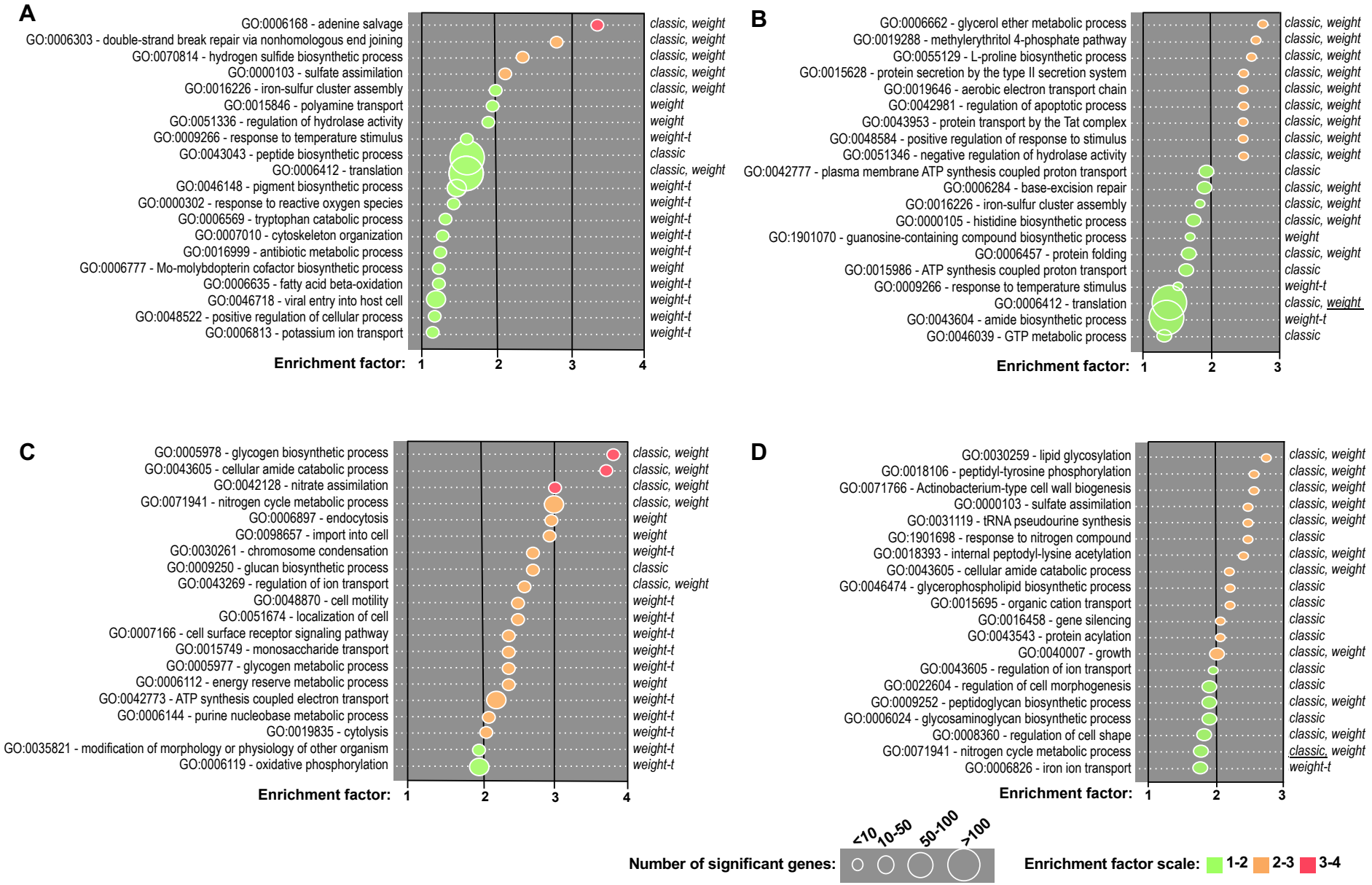
A
GO:0006168 - adenine salvage
GO:0006303 - double-strand break repair via nonhomologous end joining
GO:0070814 - hydrogen sulfide biosynthetic process
GO:0000103 - sulfate assimilation
GO:0016226 - iron-sulfur cluster assembly
GO:0015846 - polyamine transport
GO:0051336 - regulation of hydrolase activity
GO:0009266 - response to temperature stimulus
GO:0043043 - peptide biosynthetic process
GO:0006412 - translation
GO:0046148 - pigment biosynthetic process
GO:0000302 - response to reactive oxygen species
GO:0006569 - tryptophan catabolic process
GO:0007010 - cytoskeleton organization
GO:0016999 - antibiotic metabolic process
GO:0006777 - Mo-molybdopterin cofactor biosynthetic process
GO:0006635 - fatty acid beta-oxidation
GO:0046718 - viral entry into host cell
GO:0048522 - positive regulation of cellular process
GO:0006813 - potassium ion transport
classic, weight
classic, weight
classic, weight
classic, weight
classic, weight
weight
weight
weight-t
classic
classic, weight
weight-t
weight-t
weight-t
weight-t
weight-t
weight
weight-t
weight-t
weight-t
weight-t
Enrichment factor:
1
2
3
4
B
GO:0006662 - glycerol ether metabolic process
GO:0019288 - methylerythritol 4-phosphate pathway
GO:0055129 - L-proline biosynthetic process
GO:0015628 - protein secretion by the type II secretion system
GO:0019646 - aerobic electron transport chain
GO:0042981 - regulation of apoptotic process
GO:0043953 - protein transport by the Tat complex
GO:0048584 - positive regulation of response to stimulus
GO:0051346 - negative regulation of hydrolase activity
GO:0042777 - plasma membrane ATP synthesis coupled proton transport
GO:0006284 - base-excision repair
GO:0016226 - iron-sulfur cluster assembly
GO:0000105 - histidine biosynthetic process
GO:1901070 - guanosine-containing compound biosynthetic process
GO:0006457 - protein folding
GO:0015986 - ATP synthesis coupled proton transport
GO:0009266 - response to temperature stimulus
GO:0006412 - translation
GO:0043604 - amide biosynthetic process
GO:0046039 - GTP metabolic process
classic, weight
classic, weight
classic, weight
classic, weight
classic, weight
classic, weight
classic, weight
classic, weight
classic, weight
classic
classic, weight
classic, weight
classic, weight
weight
classic, weight
classic
weight-t
classic, weight
weight-t
classic
Enrichment factor:
1
2
3
C
GO:0005978 - glycogen biosynthetic process
GO:0043605 - cellular amide catabolic process
GO:0042128 - nitrate assimilation
GO:0071941 - nitrogen cycle metabolic process
GO:0006897 - endocytosis
GO:0098657 - import into cell
GO:0030261 - chromosome condensation
GO:0009250 - glucan biosynthetic process
GO:0043269 - regulation of ion transport
GO:0048870 - cell motility
GO:0051674 - localization of cell
GO:0007166 - cell surface receptor signaling pathway
GO:0015749 - monosaccharide transport
GO:0005977 - glycogen metabolic process
GO:0006112 - energy reserve metabolic process
GO:0042773 - ATP synthesis coupled electron transport
GO:0006144 - purine nucleobase metabolic process
GO:0019835 - cytolysis
GO:0035821 - modification of morphology or physiology of other organism
GO:0006119 - oxidative phosphorylation
classic, weight
classic, weight
classic, weight
classic, weight
weight
weight
weight-t
classic
classic, weight
weight-t
weight-t
weight-t
weight-t
weight-t
weight
weight-t
weight-t
weight-t
weight-t
weight-t
Enrichment factor:
1
2
3
4
D
GO:0030259 - lipid glycosylation
GO:0018106 - peptidyl-tyrosine phosphorylation
GO:0071766 - Actinobacterium-type cell wall biogenesis
GO:0000103 - sulfate assimilation
GO:0031119 - tRNA pseudouridine synthesis
GO:1901698 - response to nitrogen compound
GO:0018393 - internal peptidyl-lysine acetylation
GO:0043605 - cellular amide catabolic process
GO:0046474 - glycerophospholipid biosynthetic process
GO:0015695 - organic cation transport
GO:0016458 - gene silencing
GO:0043543 - protein acylation
GO:0040007 - growth
GO:0043605 - regulation of ion transport
GO:0022604 - regulation of cell morphogenesis
GO:0009252 - peptidoglycan biosynthetic process
GO:0006024 - glycosaminoglycan biosynthetic process
GO:0008360 - regulation of cell shape
GO:0071941 - nitrogen cycle metabolic process
GO:0006826 - iron ion transport
classic, weight
classic, weight
classic, weight
classic, weight
classic, weight
classic
classic, weight
classic, weight
classic
classic
classic
classic
classic, weight
classic
classic
classic, weight
classic
classic, weight
classic, weight
weight-t
Enrichment factor:
1
2
3
Number of significant genes:
<10
10-50
50-100
>100
Enrichment factor scale:
1-2
2-3
3-4

Figure 3

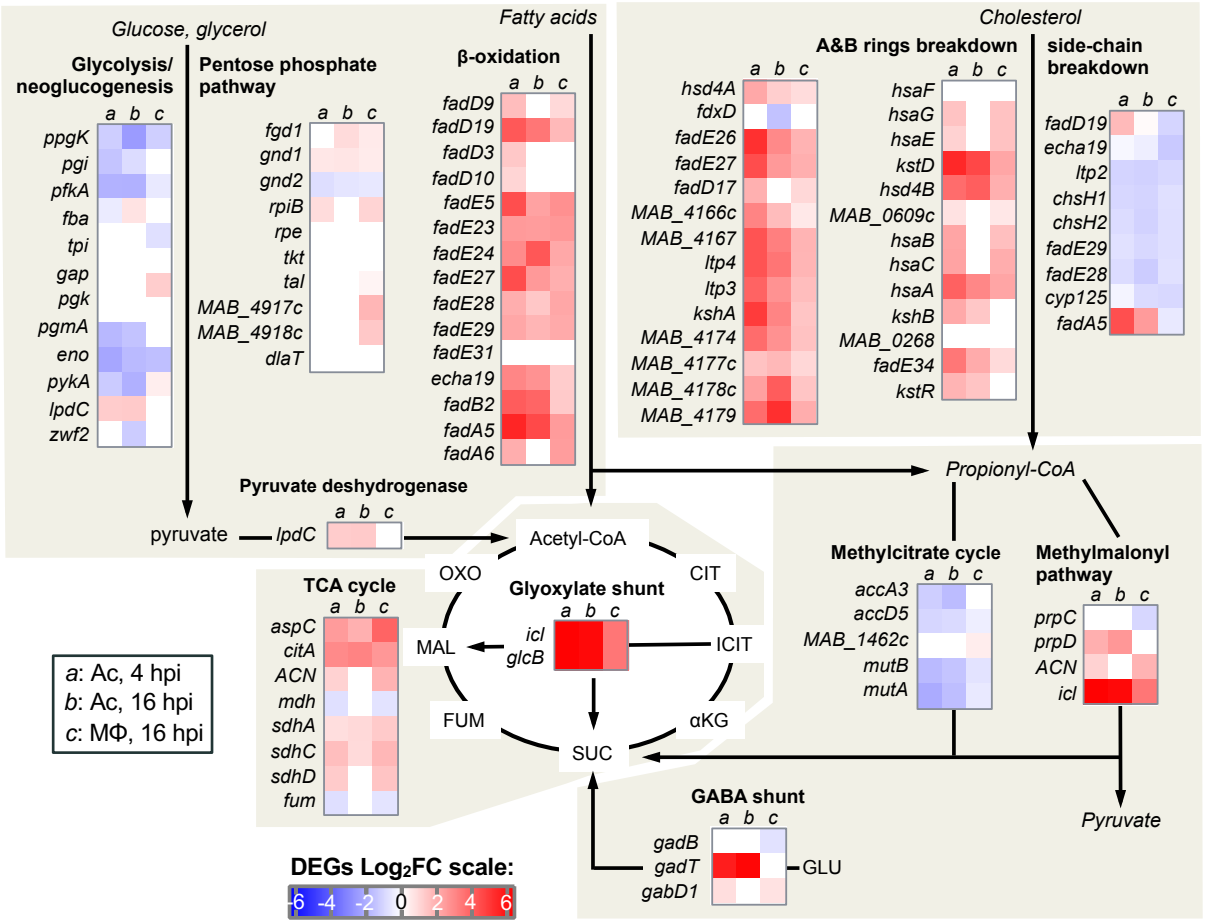
Glucose, glycerol
Fatty acids
Cholesterol
Glycolysis/ neoglucogenesis
Pentose phosphate pathway
β-oxidation
A&B rings breakdown
side-chain breakdown
a b c
ppgK
pgi
pfkA
fba
tpi
gap
pgk
pgmA
eno
pykA
lpdC
zwf2
fgd1
gnd1
gnd2
rpiB
rpe
tkt
tal
MAB_4917c
MAB_4918c
dlaT
fadD9
fadD19
fadD3
fadD10
fadE5
fadE23
fadE24
fadE27
fadE28
fadE29
fadE31
echa19
fadB2
fadA5
fadA6
hsd4A
fdxD
fadE26
fadE27
fadD17
MAB_4166c
MAB_4167
ltp4
ltp3
kshA
MAB_4174
MAB_4177c
MAB_4178c
MAB_4179
hsaF
hsaG
hsaE
kstD
hsd4B
MAB_0609c
hsaB
hsaC
hsaA
kshB
MAB_0268
fadE34
kstR
fadD19
echa19
ltp2
chsH1
chsH2
fadE29
fadE28
cyp125
fadA5
Pyruvate deshydrogenase
pyruvate
lpdC
Acetyl-CoA
Propionyl-CoA
OXO
CIT
ICIT
αKG
SUC
FUM
MAL
Glyoxylate shunt
icl
glcB
TCA cycle
aspC
citA
ACN
mdh
sdhA
sdhC
sdhD
fum
Methylcitrate cycle
accA3
accD5
MAB_1462c
mutB
mutA
Methylmalonyl pathway
prpC
prpD
ACN
icl
Pyruvate
GABA shunt
gadB
gadT
gabD1
GLU
a: Ac, 4 hpi
b: Ac, 16 hpi
c: MΦ, 16 hpi
DEGs Log2FC scale:
-6 -4 -2 0 2 4 6

Figure 4

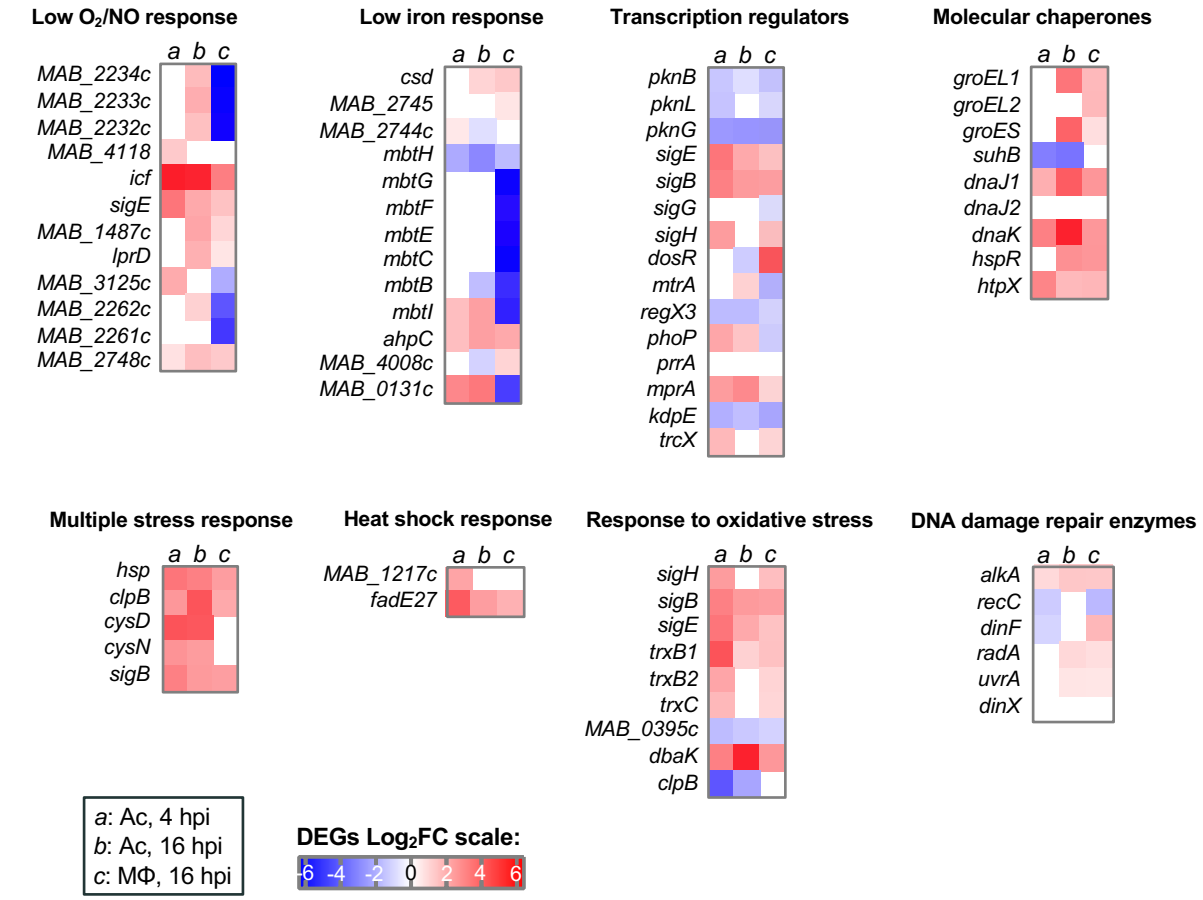
Low O2/NO response
a b c
MAB_2234c
MAB_2233c
MAB_2232c
MAB_4118
icf
sigE
MAB_1487c
lprD
MAB_3125c
MAB_2262c
MAB_2261c
MAB_2748c
Low iron response
a b c
csd
MAB_2745
MAB_2744c
mbtH
mbtG
mbtF
mbtE
mbtC
mbtB
mbtI
ahpC
MAB_4008c
MAB_0131c
Transcription regulators
a b c
pknB
pknL
pknG
sigE
sigB
sigG
sigH
dosR
mtrA
regX3
phoP
prrA
mprA
kdpE
trcX
Molecular chaperones
a b c
groEL1
groEL2
groES
suhB
dnaJ1
dnaJ2
dnaK
hspR
htpX
Multiple stress response
a b c
hsp
clpB
cysD
cysN
sigB
Heat shock response
a b c
MAB_1217c
fadE27
Response to oxidative stress
a b c
sigH
sigB
sigE
trxB1
trxB2
trxC
MAB_0395c
dbaK
clpB
DNA damage repair enzymes
a b c
alkA
recC
dinF
radA
uvrA
dinX
a: Ac, 4 hpi
b: Ac, 16 hpi
c: MΦ, 16 hpi
DEGs Log2FC scale:
-6 -4 -2 0 2 4 6

Figure 5

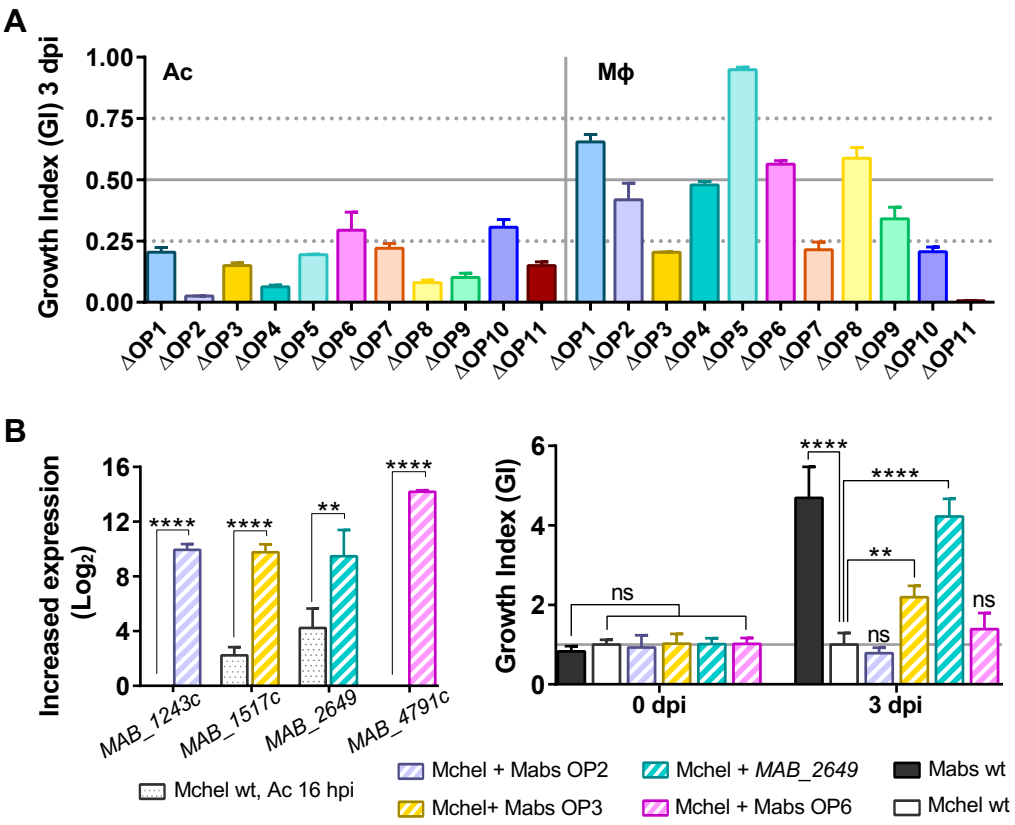
A
Growth Index (GI) 3 dpi
1.00
0.75
0.50
0.25
0.00
Ac
Mϕ
ΔOP1
ΔOP2
ΔOP3
ΔOP4
ΔOP5
ΔOP6
ΔOP7
ΔOP8
ΔOP9
ΔOP10
ΔOP11
B
Increased expression (Log2)
16
12
8
4
0
****
****
**
****
MAB_1243c
MAB_1517c
MAB_2649
MAB_4791c
Mchel wt, Ac 16 hpi
Growth Index (GI)
6
4
2
0
ns
****
****
**
ns
ns
0 dpi
3 dpi
Mchel + Mabs OP2
Mchel + MAB_2649
Mabs wt
Mchel+ Mabs OP3
Mchel + Mabs OP6
Mchel wt

Figure 6

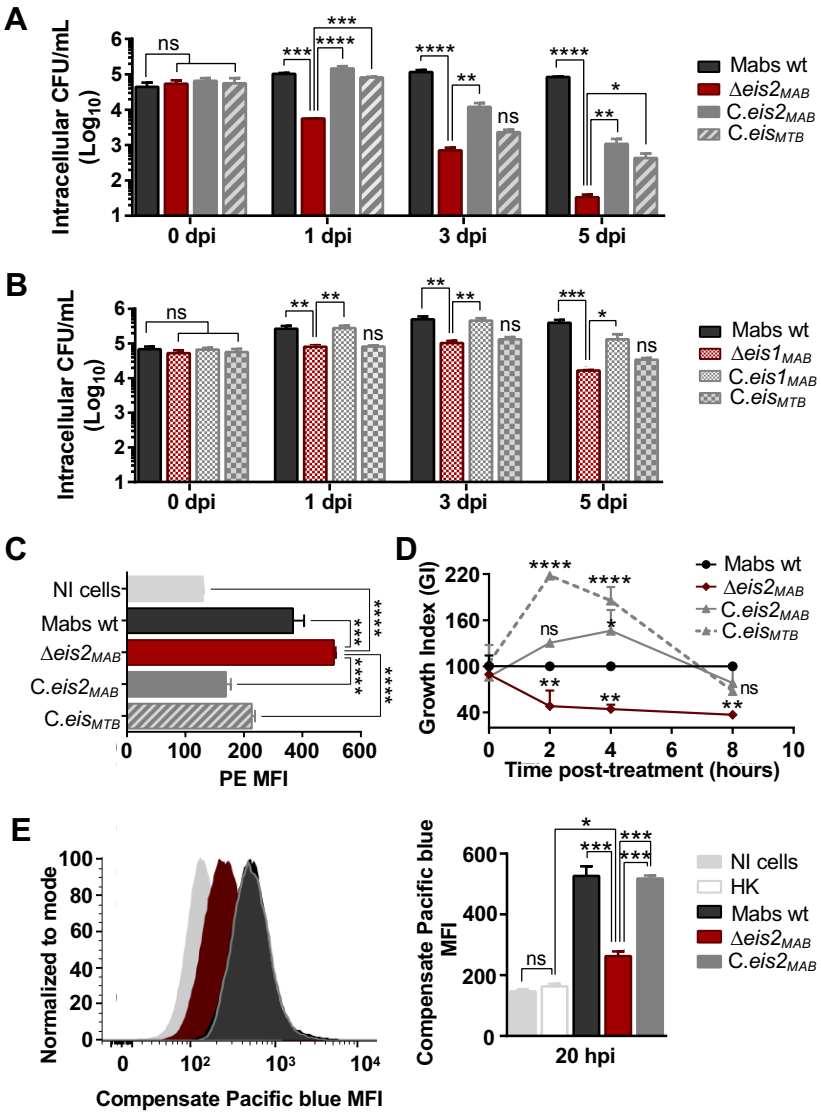
A
Intracellular CFU/mL (Log10)
0 dpi
1 dpi
3 dpi
5 dpi
Mabs wt
Δeis2MAB
C.eis2MAB
C.eisMTB
B
Intracellular CFU/mL (Log10)
Δeis1MAB
C.eis1MAB
C.eisMTB
C
NI cells
Mabs wt
Δeis2MAB
C.eis2MAB
C.eisMTB
PE MFI
D
Growth Index (GI)
Time post-treatment (hours)
E
Normalized to mode
Compensate Pacific blue MFI
Compensate Pacific blue MFI
20 hpi
NI cells
HK

882 **Table 1: Regulation of *M. abscessus* mycolate synthesis operon in Ac and Mϕ.**

Mma gene	Encoded protein	Mabs gene	FC Ac 4 hpi	FC Ac 16 hpi	FC Mϕ 16 hpi
MYCMA_RS13950	Acyl carrier protein	*MAB_2027*	-3.28	-2.91	0.00
MYCMA_RS13945	3-oxoacyl-ACP synthase (Kas B)	*MAB_2028*	-2.68	-2.24	0.00
MYCMA_RS13940	Beta-ketoacyl synthase	*MAB_2029*	-2.95	-4.48	0.00
MYCMA_RS13935	3-oxoacyl-ACP synthase (Kas A)	*MAB_2030*	-3.80	-3.15	0.00
MYCMA_RS13930	Beta-ketoacyl synthase	*MAB_2031*	-2.92	0	-1.60
MYCMA_RS13925	3-oxoacyl-ACP reductase	*MAB_2032*	-2.16	0	-1.85
MYCMA_RS13920	Thioesterase	*MAB_2033*	-2.09	0	0.00
MYCMA_RS13915	Malonyl CoA-ACP transacylase	*MAB_2034*	-2.09	0	0.00
MYCMA_RS13910	Acyltransferase	*MAB_2035*	0	0	0.00
MYCMA_RS13905	Membrane protein (MmpS)	*MAB_2036*	-1.16	0	-1.06
MYCMA_RS13900	Hypothetical protein (MmpL)	*MAB_2037*	-0.68	-0.86	0.00
MYCMA_RS13895	Transporter	*MAB_2038*	0	0	0.00
MYCMA_RS13890	Lipase (LipH)	*MAB_2039*	0	0.86	-0.72

883

884

885 **Table 2: Deleted operons in *M. abscessus* ATCC19977.**

Operon ID	Mabs gene	Protein encoded	IP5 motif analysis on hypothetical proteins
OP1 (2231455)	*MAB_4664*	Hypothetical protein	No IPR
OP2 (395711)	*MAB_1242c*	Hypothetical protein	No IPR
	MAB_1243c	Hypothetical protein	IPR035568: ABC transporter. FecCD/TroCD-like
	MAB_1244c	Hypothetical protein	No IPR
	MAB_1245c	Hypothetical protein	No IPR
	MAB_1246c	Hypothetical protein	No IPR
	MAB_1247c	Hypothetical protein	IPR005531: Alkaline shock protein Asp23
OP3 (2230454)	*MAB_1517c*	Probable O-methyltransferase Omt	
OP4 (396003)	*MAB_2649*	Putative membrane protein. MmpS family	
	MAB_2650	Putative membrane protein. MmpL family	
OP5 (2231454)	*MAB_4663*	Hypothetical protein	No IPR
OP6 (2231514)	*MAB_4791c*	Hypothetical protein	Twin-arginine translocation pathway. Signal sequence
OP7 (2229980)	*MAB_0086*	Taurine catabolism dioxygenase	
OP8 (395598)	*MAB_0734*	Hypothetical protein	Leukocidin/porin MspA superfamily (036435)
OP9 (396109)	*MAB_3132c*	Membrane protein	No IPR
	MAB_3133c	Hemin transporter	
	MAB_3134c	Transcriptional regulator	
OP10 (2231416)	*MAB_4509c*	Hypothetical protein	No IPR
OP11 (22311420)	*MAB_4532c*	Hypothetical protein	N-acetyltransferase Eis (016181)

886